Industrial Crops and Products 90 (2016) 9–27

Contents lists available at ScienceDirect

Industrial Crops and Products

journal homepage: www.elsevier.com/locate/indcrop

Ulex europaeus: from noxious weed to source of valuable isoflavones and flavanones

Vítor Spínola [a], Eulogio J. Llorent-Martínez [b], Sandra Gouveia-Figueira [c], Paula C. Castilho [a,*]

[a] CQM—Centro de Química da Madeira, Universidade da Madeira, Campus da Penteada, 9020-105 Funchal, Portugal
[b] University of Castilla-La Mancha, Regional Institute for Applied Chemistry Research (IRICA), Ciudad Real 13071, Spain
[c] Department of Chemistry, Umeå University, 901 87 Umeå, Sweden

ARTICLE INFO

Article history:
Received 24 February 2016
Received in revised form 27 May 2016
Accepted 3 June 2016

Keywords:
Ulex europaeus
Isoflavones
Liquiritigenin
HPLC-ESI/MS^n analysis
Antioxidant activity
Digestive enzymes inhibition

ABSTRACT

The screening and quantification of the main phenolic compounds in leaves and flowers of *Ulex europaeus* (gorse) was carried out by high-performance liquid chromatography with electrospray ionization mass spectrometric detection (HPLC-ESI–MS^n) after ultrasound-assisted extraction with methanol. About 98% of compounds corresponded to flavonoids, distributed as flavonols, flavones, isoflavones and flavanones. Flavonols were mainly quercetin glucosides; most of the found flavones were apigenin derivatives and the isoflavone group was dominated by glycitin. The flavanone group was composed mainly of liquiritigenin derivatives, substances usually found in liquorice (*Glycyrrhiza* ssp) and associated with high pharmacological relevance; in *Ulex* they represent about 25% of total polyphenols content. Phenolic acids and saponins were also detected, as minor components. *In vitro* antioxidant activity (nitric oxide, superoxide assays, ABTS and DPPH assays) of leaves and flowers, and their inhibitory effects towards digestive enzymes related to carbohydrate metabolism (α-glucosidase and α-amylase) were also studied.

1. Introduction

The genus Ulex L. (Fabaceae) is well represented in Portugal, where ten species are recognized and some of them are endemic (Máximo et al., 2002a, 2002b). *Ulex europaeus* L. (gorse, furze or whin) is native mainly to Western Europe and was introduced in the early 19th century in Madeira Island (Portugal), where it rapidly became invasive. It blooms all year, but mainly between January and June (Press and Short, 1994). The flowers have been used in folk medicine as infusions with sugar cane liquor as antirheumatic, and also for the treatment of liver diseases, diabetes, asthma, and hypertension (Rivera and Obón, 1995), whereas leaves were used as forage shrub considering their high crude protein content (Tolera et al., 1997). Previous reports stated that *Ulex* species are a rich source of isoflavonoids (in particular isoflavones and pterocarpans) with relevant antifungal activity, insecticide or cytotoxic effects (Máximo et al., 2002a, 2002b, 2000; Veitch, 2007). Isoflavones are considered to belong to the "phytoestrogen" class, due to their similar effects to mammalian estrogens (Veitch, 2013). Genistein, daidzein and glycitein are considered the most important isoflavones, due to their varied biological actions, dependent on their aglycone and conjugated forms (Vitale et al., 2013). These isoflavones are abundant in soybeans and related products and in other edible Fabaceae, such as lupin and fava beans. Flavanones are intermediates in the biosynthesis of other flavonoids and are present in most plants, but accumulate particularly in Asteraceae and Fabaceae. Flavanones and their isomeric chalcones interconvert enzymatically in most of these species, so it is common to find both types of structures.

Naringenin and liquiritigenin are the flavanones that present the most interesting biological activities. In particular, liquiritigenin and its conjugated forms display antioxidant, anti-inflammatory and antitumor activities and neuroprotective effects (Peng et al., 2015). Licorice root is the main commercial source of liquiritigenin derivatives (Tian et al., 2009) and most publications describing the bioactivity of these compounds refer to isolates from liquorice extracts. Harborne (Harborne, 1972) reported the presence of

Abbreviations: DE, dry extract; HPLC-ESI–MS^n, high-performance liquid chromatography with electrospray ionization mass spectrometric detection; NADHβ, nicotinamide adenine dinucleotide reduced; NBT, nitroblue tetrazolium chloride; NO, nitric oxide; PCA, Principal component analysis; PMS, phenazinemethosulfate; *p*NPG, pnitrophenyl-α-D-glucopyranoside; SO, superoxide; TFC, total flavonoid content; TIPC, total individual phenolic content; TPC, total phenolic content.

* Corresponding author.
E-mail addresses: castilho@uma.pt, alixstone@gmail.com (P.C. Castilho).

http://dx.doi.org/10.1016/j.indcrop.2016.06.007
0926-6690/

isoliquiritigenin glucosides in the flowers of *Ulex* as early as 1962. However, the screening and quantitative relevance of these components of *Ulex* is not described. The phytochemical composition of *Ulex europaeus* L. is here determined by means of an HPLC-ESI–MS^n method. The quantification of the main polyphenols from leaves and flowers was also carried out, as well as their *in vitro* antioxidant activities (ABTS, DPPH, nitric oxide and superoxide assays) and inhibitory effects towards digestive enzymes related to carbohydrate metabolism (α-glucosidase and α-amylase).

2. Experimental

2.1. Chemicals and reagents

All reagents and standards were of analytical reagent grade unless stated otherwise. Folin-Ciocalteu's phenol reagent (FCR), sodium chloride, potassium chloride, gallic acid (>98%), quercetin hydrated (>99%) and potassium acetate (>99.5%) were obtained from Panreac (Barcelona, Spain). 6-hydroxy-2,5,7,8-tetramethylchroman-2-carboxylic acid (Trolox), 2,2′azinobis-(3-ethylbenzthiazoline-6-sulfonic acid) (ABTS) and 2,2-diphenyl-1-picrylhydrazyl (DPPH) and methanol (99.9%) were obtained from Fluka (Lisbon, Portugal). Kaempferol (> 99%) was purchased from Acros Organics (Geel, Belgium). Apigenin (≥99%) was obtained from Extrasynthese (Genay, France). *N*-(1-naphthyl)ethylene-diamine dihydrochloride (≥98%), phenazinemethosulfate (PMS, ≥90%), sulfanilamide (≥99%), β-nicotinamide adenine dinucleotide reduced (NADH, ≥94%), caffeic acid (≥98%), protocatechuic acid (98%, HPLC), rutin (≥95%), potassium persulfate (99%), sodium carbonate (100%), α-glucosidase from *Saccharomyces cerevisiae* (type I), α-amylase from porcine pancreas (type VI-B), *p*-nitrophenyl-α-D-glucopyranoside (pNPG) and formic acid (98%) were purchased from Sigma-Aldrich (St. Louis, MO, USA). Nitroblue tetrazolium chloride (NBT, 90%) was obtained from Acros Organics and o-phosphoric acid (85%) from BDH AnalaR. Hydrochloric acid (37%) was purchased from Fischer Chemicals (Leicestershire, UK). Liquiritin (≥98%) was obtained from Biopurify phytochemicals LTD (Chengdu, China). Potato starch (p.a.), potassium iodate (99.5%), sodium nitroprusside (99%), and ethylenediaminetetraacetic acid (EDTA; >99%) were obtained from Merck (Darmstadt, Germany). Acarbose (Acarbose Generis®) was purchased from a drug store. LC–MS grade acetonitrile (CH_3CN, 99%) (LabScan; Dublin, Ireland) and ultrapure water (Milli-Q Waters purification system; Millipore; Milford, MA, USA) were used for the HPLC–MS analyses.

2.2. Sample preparation and extraction of phenolic compounds

Samples of *U. europaeus* were collected in the wild at two different locations of Madeira Island (Funchal and Machico) in January 2015. For analysis, leaves were separated from flowers, lyophilized to dryness (Alpha 1-2 LD plus freeze dryer, CHRIST), ground to powder in a mechanic grinder, and stored at −20 °C. Then, 1 g of dried leaves was extracted with 25 mL of methanol using a sonicator Bandelin Sonorex (Germany) at 35 Hz and 200 W for 60 min (room temperature). Chlorophylls were removed by adsorption on activated charcoal, and extracts were filtered and concentrated to dryness under reduced pressure in a rotary evaporator (Buchi Rotavapor R-114; USA) at 40 °C. The resulting extracts were stored at 4 °C until analysis.

2.3. Chromatographic conditions

The HPLC analysis was performed on a Dionex ultimate 3000 series instrument (Thermo Scientific Inc.) coupled to a binary pump, an autosampler and a column compartment (kept at 20 °C). Separation was carried out in a Phenomenex Gemini C_{18} column (5 μm, 250 × 3.0 mm i.d.) using a mobile phase composed by CH_3CN (A) and water/formic acid (0.1%, v/v) at a flow rate of 0.4 mL min^{-1}. The following gradient program was used: 20% A (0 min), 25% A (10 min), 25% A (20 min), 50% A (40 min), 100% A (42–47 min) and 20% A (49–55 min). Sample solutions (5 mg mL^{-1}) were prepared by dissolving the dried extract in the initial HPLC mobile phase. After filtration through 0.45 μm PTFE membrane filters, 5 μL was injected.

For HPLC-ESI–MS^n analysis, a Bruker Esquire model 6000 ion trap mass spectrometer (Bremen, Germany) with an ESI source was used. MS^n analysis was performed in negative and positive modes and scan range was set at *m/z* 100–1000 with a speed of 13,000 Da/s. The ESI conditions were as follows: drying and nebulizer gas (N_2) flow rate and pressure, 10 mL min^{-1} and 50 psi; capillary temperature, 325 °C; capillary voltage, 4.5 keV; collision gas (He) pressure and energy, 1×10^{-5} mbar and 40 eV. The acquisition of MS^n data was made in auto MS^n mode, with an isolation width of 4.0 *m/z*, and a fragmentation amplitude of 1.0 V (MS^n up to MS^4). Esquire control software was used for the data acquisition and Data Analysis for processing.

2.4. Quantification of phenolic compounds

For this quantitative analysis, one polyphenol was selected as the standard for each group, being used to calculate individual concentrations by HPLC-DAD. Caffeic and gallic acids were used for hydroxycinnamic and hydroxybenzoic acids, respectively. Quercetin, apigenin, and liquiritin were the standards used for the flavonols, flavones, and flavanones, respectively. Stock standard solutions (1000 mg L^{-1} each) were prepared in methanol, and calibration curves were prepared by diluting the stock solutions with the initial mobile phase. Six concentrations (5–100 mg L^{-1}) were used for the calibration, plotting peak area versus concentration ($R^2 \geq 0.967$ in all cases). Total individual phenolic contents (TIPC) were defined as the sum of the quantified phenolic compounds.

2.5. Total phenolic and flavonoid contents and in vitro antioxidant assays

2.5.1. Total phenolic content (TPC)

The TPC was determined following a previous described protocol (Spínola et al., 2014): 50 μL aliquots (5 mg of dry extract, DE, per mL of methanol) were mixed with 1.25 mL of FCR (diluted 1:10 with water) and 1 mL of 7.5% Na_2CO_3 aqueous solution. After 30 min in the dark at room temperature, the absorbance was measured at 765 nm in a Perkin Elmer UV–vis Lambda 2 spectrophotometer (Oberlingen, Germany). The amounts of total phenolics were expressed as mg of gallic acid equivalents (GAE)/100 g of DE.

2.5.2. Total flavonoid content (TFC)

The total flavonoid content was determined as follows (Spínola et al., 2014): 0.5 mL of methanolic solutions (2.5 mg mL^{-1}) was mixed with 1.5 mL of methanol, 2.8 mL of distilled water, 0.1 mL of CH_3COOK (1 mol L^{-1}), and 0.1 mL of $AlCl_3.6H_2O$ (10% in MeOH). The absorbance was measured at 415 nm after 30 min of reaction (room temperature, in the dark). The final results were expressed as mg of rutin equivalent (RUE)/100 g DE.

2.5.3. ABTS radical scavenging activity

Determination of antioxidant activity was based on a previous procedure (Spínola et al., 2014): 40 μL of methanolic solution (5 mg mL^{-1}) was added to 1.96 mL of $ABTS^{\bullet+}$ solution (diluted in PBS pH 7.4 until the absorbance is 0.700 ± 0.021). The reduction of absorbance at 734 nm was measured during 6 min, and the results were expressed as μmol of Trolox equivalent (TE)/100 g DE.

2.5.4. DPPH radical scavenging activity

The DPPH assay followed a previously reported method (Spínola et al., 2014): 100 μL of methanolic solution (5 mg mL^{-1}) was added to 3.5 mL of DPPH radical solution (0.06 mol L^{-1}). Absorbance was measured at 516 nm, after 30 min of reaction in the dark (room temperature) andresults were expressed as μmol TE/100 g DE.

2.5.5. Nitric oxide (NO) scavenging activity

The antiradical activity was determined spectrophotometrically using a model Victor^3 microtiter reader (Perkin-Elmer, Ueberlingen, Germany), with slight modifications from a previous procedure (Sousa et al., 2008). Briefly, 50 μL of 20 mM sodium nitroprusside was mixed with 50 μL of sample (5 mg mL^{-1}) for 60 min, at room temperature, under light. All solutions were prepared in 0.1 M phosphate buffer (pH 7.4). After incubation, 50 μL of Griess reagent (1% sulfanilamide and 0.1% naphthylethylenediamine dihydrochloride in 2% phosphoric acid), was added to each well. Then, the absorbance was read at 550 nm and the results were expressed as μmol TE/100 g DE.

2.5.6. Superoxide radical (SO) scavenging activity

Superoxide radicals were generated by the NADH/PMS system according to a described procedure (Ewing and Janero, 1995): 25 μL of sample (5 mg mL^{-1}) was mixed with 200 μL of a solution composed by 0.1 mmol L^{-1} EDTA, 62 μmol L^{-1} NBT and 98 μmol L^{-1} NADH. The reaction was initiated by the addition of 25 μL of 33 μmol L^{-1} PMS (containing 0.1 mM EDTA) to each well. All solutions were prepared in 0.1 M phosphate buffer (pH 7.4). The absorbance was read at 550 nm (Victor^3 microtiter reader; Perkin-Elmer, Ueberlingen, Germany) and the results were expressed as μmol TE/100 g DE.

2.6. In vitro *inhibition of digestive enzymes*

2.6.1. α-Glucosidase inhibition assay

In a 96-well plate, 50 μL of extract solution was combined with 50 μL of enzyme solution and incubated for 20 min in the dark at room temperature (Podsędek et al., 2014). A gradient of concentrations was prepared via serial dilutions of the extracts in distilled water. The reaction was initiated by adding 50 μL of 5 mmol L^{-1} *p*-NPG solution in 0.1 mol L^{-1} phosphate buffer (pH 7.0). The mixture was incubated at 37 °C, in the dark, for 20 min. Finally, 100 μL of 0.1 mol L^{-1} Na_2CO_3 solution was added and the absorbance was read at 405 nm. Acarbose was used as positive control. The inhibitory activity was expressed as the IC50 value (mg mL^{-1} of DE), determined from the least-squares regression line of the logarithmic concentrations plotted against percentage inhibition.

2.6.2. α-Amylase inhibition assay

Twenty microliters of extract solution and 40 μL of 2 g L^{-1} starch solution were mixed with 20 μL of α-amylase (in phosphate buffer 7.0) (Podsędek et al., 2014). A gradient of concentrations was prepared via serial dilutions of the extracts in distilled water. After incubation at 37 °C for 20 min in the dark, the reaction was stopped by the addition of 80 μL of HCl followed by 100 μL of 5 mmol L^{-1} I_2 (in 5 mmol L^{-1} KI), and the absorbance was read at 620 nm. Acarbose was used as positive control. The inhibitory activity was expressed as the IC50 value, as described previously.

2.7. Statistical analysis

All samples were assayed in triplicate ($n = 3$) and results are given as the means ± standard deviations. Data were analyzed by means of a one-way ANOVA using SPSS for Windows, IBM SPSS Statistics 20 (SPSS, Inc., USA). A value of $p < 0.05$ was considered statistically significant. Principal component analysis (PCA) was applied to the autoscaled concentrations of the determined polyphenols in *Ulex* samples from different locations, using an R statistical software package.

3. Results and discussion

The analysis of the phenolic composition of *U. europaeus* leaves and flowers by HPLC-ESI–MS^n was carried out in positive and negative ionization modes. Two independent assays were performed for each sample, and no relevant variations were observed concerning the nature and relative intensities of the detected fragments. The base peak chromatograms of the methanolic extracts are shown in Fig. 1 (only the most abundant compounds are numbered for the sake of clarity).

An essential step was to determine the molecular ion of each compound. In the negative ionization mode (ESI$^-$) MS^1 spectrum, the most intense peak usually corresponded to the deprotonated molecular ion [M−H]$^-$, although sometimes formic adducts were observed ([M−H + HCOOH]$^-$). The mass spectra of the conjugated phenolic compounds showed the aglycone ion as result of the loss of sugar moieties like hexosyl or pentosyl (−162, −132 Da, respectively). Mass spectra data from the positive ionization (ESI$^+$) mode was only used for confirmation purposes. Compounds were numbered by their order of elution. The structures of the most relevant compounds are shown in Fig. 2.

3.1. Phenolic acids

Compound **6** with the [M−H]$^-$ion at *m/z* 461 and MS^2 base peak at *m/z* 167 was tentatively characterized as vanillic acid 4-*O*-pentosylhexoside (Maier et al., 2015).

Compounds **10, 20** and **32** exhibited the [M−H]$^-$ ions at *m/z* 341, and suffered the neutral loss of 162 Da (hexoside) yielding an MS^2 base peak at *m/z* 179. The MS^3 [341 → 179] fragmentation produced an ion at *m/z* 135, indicating that the ion at *m/z* 179 corresponded to caffeic acid (compared with a commercial standard). Therefore, they were tentatively identified as caffeic acid-*O*-hexoside. Compound **7**, with [M−H]$^-$ at *m/z* 503, displayed a fragment ion at *m/z* 341 (loss of 162 Da), and its MS^3 fragmentation was similar to compound **10**, so this compound was tentatively identified as caffeic acid-*O*-dihexoside. Compounds **63** and **113** also displayed MS^n fragment ions at *m/z* 179 and 135 and were tentatively characterized as caffeic acid derivatives.

Compound **23**, with [M−H]$^-$ at *m/z* 651, suffered the neutral loss of 326 Da, yielding a fragment ion at *m/z* 325. The ion at *m/z* 325 exhibited the typical fragmentation of *p*-coumaric acid-*O*-hexoside, with MS^3 [651 → 325] fragment ions at *m/z* 163 and 119 (Sánchez-Rabaneda et al., 2003). It was tentatively characterized as a dimer of *p*-coumaric acid hexoside. Compound **11** was tentatively identified as coumaric acid-*O*-hexoside (formate adduct). Compounds **46** and **124** also displayed the typical fragmentation pattern of coumaric acid, so they were tentatively characterized as derivatives.

Several derivatives of ferulic acid were observed in the analyzed samples. Compound **16** was tentatively identified as a dimer of ferulic acid-*O*-hexoside. Compound **26**, with [M−H]$^-$ at *m/z* 487, suffered neutral losses of 132 Da (pentoside) and 132 + 162 Da (pentoside + hexoside), yielding fragments at *m/z* 355 and 193; it was tentatively characterized as ferulic acid-*O*-pentosylhexoside. Compounds **31**, **37**, and **42** displayed the deprotonated molecular ion at *m/z* 355. Compound **31** suffered the neutral loss of 162 Da (hexoside) to yield the MS^2 base peak at *m/z* 193, which displayed the fragment ions characteristic of ferulic acid at *m/z* 178, 149 and 134. Hence, this compound was tentatively characterized as ferulic acid-*O*-hexoside (Fang et al., 2002). Compound **37** showed a fragment ion at *m/z* 337 [M−H−18]$^-$, indicative of a 6-*C* glycoside

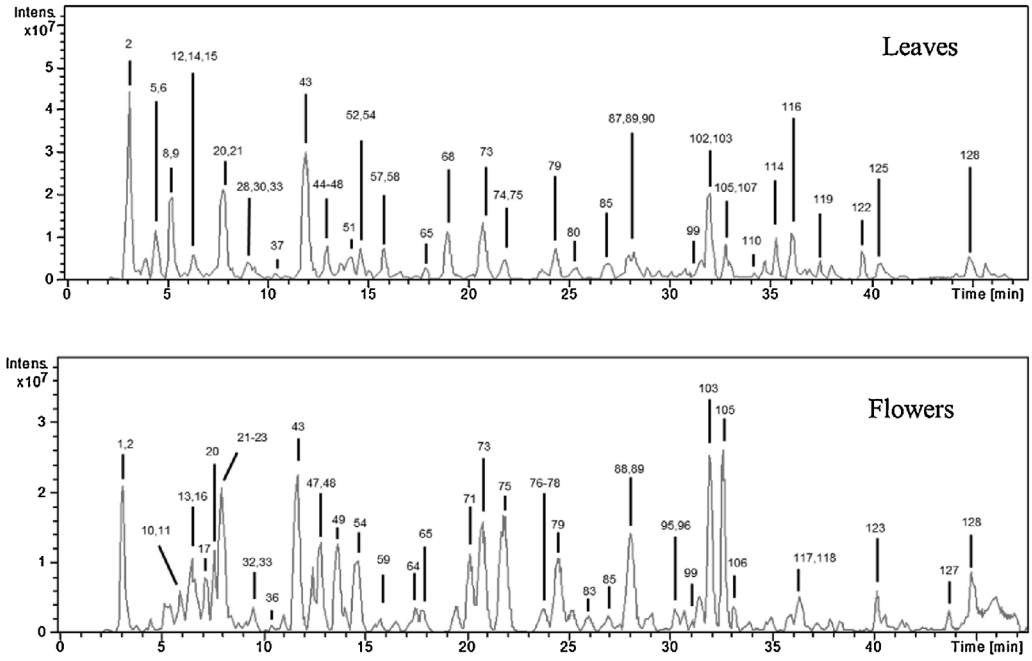

Fig. 1. HPLC-ESI/MS^n base peak chromatograms (BPC) of the methanolic extracts from *Ulex europaeus* leaves and flowers collected in Funchal.

(Waridel et al., 2001), whereas the absence of the loss of water in the spectrum of **42** indicated a 8-*C* glycoside. Hence, compounds **37** and **42** were tentatively identified as ferulic acid-6-*C*-hexoside and ferulic acid-8-*C*-hexoside, respectively. Following a similar fragmentation pattern, compound **45** was tentatively characterized as a ferulic acid-*C*-hexoside derivative (loss of 60, 90, 120, and 162 Da). Compounds **28**, **41**, and **126** could not be fully identified and were tentatively characterized as ferulic acid derivatives.

Compound **39**, with $[M-H]^-$ ion at *m*/*z* 385, exhibited MS^2 fragment ions at *m*/*z* 265 $[M-H-120]^-$, 295 $[M-H-90]^-$ and 325 $[M-H-60]^-$, characteristic of *C*-glycosides. The aglycone was observed at *m*/*z* 223. This fragmentation is consistent with the bibliographic data for sinapic acid-*C*-hexoside (Vallverdú-Queralt et al., 2014).

Compound **84** exhibited the deprotonated molecular ion at *m*/*z* 515 and was tentatively identified as 3,5-*O*-dicaffeoylquinic acid by comparison of its fragmentation with bibliographic data (Gouveia and Castilho, 2009).

3.2. Flavonoids

Compound **8**, $[M-H+HCOOH]^-$ at *m*/*z* 653, was tentatively identified as acacetin-*O*-dihexoside (formate adduct), since it suffered the neutral loss of 208 Da (hexoside + formic acid), yielding a fragment ion at *m*/*z* 445, followed by the loss of another hexoside residue (445 → 283). The aglycone was characterized as acacetin due to the fragment ion at *m*/*z* 268 (Parejo et al., 2004). The positive mode confirmed this identification, showing the 285 → 270 transition, typical from acacetin (Shi et al., 2011).

Compound **9**, with $[M-H+HCOOH]^-$ at *m*/*z* 623, suffered the sequential losses of hexoside + formic (623 → 415) and hexoside (415 → 253), yielding the aglycone daidzein at *m*/*z* 253 (Kang et al., 2007), so it was tentatively identified as daidzein-*O*-dihexoside.

Compounds **13** and **44** exhibited $[M-H]^-$ ions at *m*/*z* 625, and suffered consecutive losses of 162 Da to yield MS^n fragment ions at *m*/*z* 463 and 301. The ion at *m*/*z* 301 displayed the characteristic fragmentation pattern of quercetin (comparison with a commercial standard). Hence, these compounds were tentatively identified as quercetin-*O*-dihexoside isomers. In a similar way, compounds **56**, **71**, **89**, and **96** were tentatively identified as quercetin-*O*-hexoside isomers.

Compounds **17** and **22**, with $[M-H]^-$ at *m*/*z* 609, suffered the sequential losses of two hexosides, to produce fragment ions at *m*/*z* 447 and 285, and were tentatively identified as kaempferol-*O*-dihexoside (Ye et al., 2005). Compound **33** displayed the $[M-H]^-$ ion at *m*/*z* 449 and, after the neutral loss of 162 Da (hexoside), yielded a fragment ion at *m*/*z* 287, which was tentatively identified as dihydrokaempferol, based on the 287 → 259 transition. Hence, **33** was tentatively characterized as dihydrokaempferol-*O*-hexoside (Llorent-Martinez et al., 2015).

Compound **18** exhibited the deprotonated molecular ion at *m*/*z* 465, and suffered the neutral loss of 162 Da to yield the aglycone at *m*/*z* 303. The MS^3 [465 → 303] spectrum displayed fragment ions at *m*/*z* 177 and 125. This fragmentation pattern is consistent with taxifolin-*O*-hexoside (Hashim et al., 2013). In addition, the MS^4 spectrum provided more fragment ions described for taxifolin (dihydroquercetin) (Ye et al., 2012), confirming the identification of the aglycone.

Compound **21**, with $[M-H+HCOOH]^-$ at *m*/*z* 639, produced fragment ions at *m*/*z* 473 $[M-H-120]^-$, 431 $[M-H-162]^-$, and 269 $[M-H-162-162]^-$, yielding the aglycone at *m*/*z* 269. This fragmentation pattern has been previously described for apigenin-*C*-hexoside-*O*-hexoside (Yang et al., 2011). Compound **51** exhibited the deprotonated molecular ion at *m*/*z* 431, and suffered the neutral loss of 162 Da to yield apigenin, so it was tentatively identified as apigenin-*O*-hexoside (Qiao et al., 2011). Compound **73**, with $[M-H+HCOOH]^-$ at *m*/*z* 477, displayed similar fragmentation pattern than **51** and was also tentatively characterized as apigenin-*O*-hexoside. Compounds **80** and **90** presented MS^n fragment ions at *m*/*z* 431, 311, and 283, which are consistent with apigenin-*C*-hexoside (Qiao et al., 2011), so they were tentatively characterized as derivatives. Compound **123** was tentatively identified as the aglycone apigenin.

Compound **24** showed $[M-H+HCOOH]^-$ at *m*/*z* 507 and suffered a neutral loss of 208 Da (162 + 46 Da). Sequential fragmentations produced fragment ions at *m*/*z* 299 $[M-H-162]^-$ and 284 $[M-H-162-15]^-$. Based on literature (Ma et al., 2014), **24** was tentatively identified as 3′5,7-trihydroxyisoflavone-4′-methoxy-

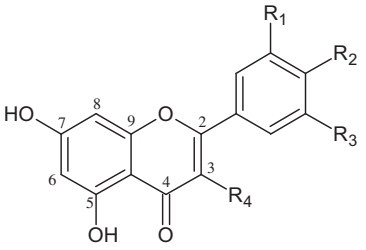

Acacetin	R_1=H ; R_2=OCH_3 ; R_3=H ; R_4=H
Apigenin	R_1=H ; R_2=OH ; R_3=H ; R_4=H
Kaempferol	R_1=H ; R_2=OH ; R_3=H ; R_4=OH
Luteolin	R_1=OH ; R_2=OH ; R_3=H ; R_4=H
Rutin	R_1=H ; R_2=OH ; R_3=OH ; R_4=O-Rutinose
Quercetin	R_1=OH ; R_2=OH ; R_3=H ; R_4=OH

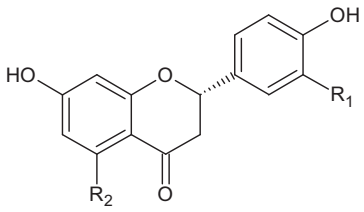

Eriodictyol	R_1=OH ; R_2=OH
Naringenin	R_1=H ; R_2=OH
Liquiritigenin	R_1=H ; R_2=H

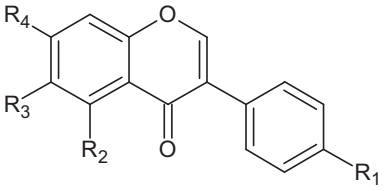

Daidzein	R_1=OH ; R_2=H ; R_3=H ; R_4=OH
Formononetin	R_1=OCH_3 ; R_2=H; R_3=H; R_4=OH
Genistein	R_1=OH; R_2=OH; R_3=H; R_4=OH
Glycitein	R_1=OH ; R_2= H ; R_3=OCH_3; ; R_4=OH
Prunetin	R_1=OH; R_2=OH ; R_3=H; R_4=OCH_3

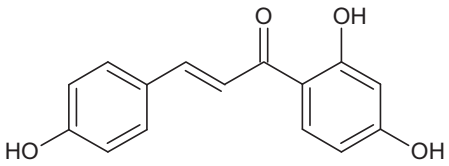

Isoliquiritigenin

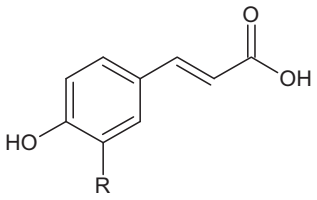

Caffeic acic	R=OH
Coumaric acid	R=H
Ferulic acid	R=OCH_3

Fig. 2. Chemical structures of the main compounds identified.

3′-*O*-β-glucopyranoside. With an extra sugar residue, compound **27** was tentatively characterized as 3′5,7-trihydroxyisoflavone-4′-methoxy-3′-*O*-β-diglucopyranoside.

Compounds **29**, **40**, and **66** were tentatively characterized as quercetin-*O*-hexoside-*O*-(malonyl)hexoside considering bibliographic data (Gouveia and Castilho, 2009). Compound **64** was identified as quercetin-*O*-rutinoside (rutin) by comparison of its fragmentation pattern with a commercial standard.

Compound **34**, with $[M-H]^-$ at *m*/*z* 611, suffered consecutive losses of two hexosides, to yield the aglycone at *m*/*z* 287. This aglycone was characterized as eriodictyol considering its main fragment ion at *m*/*z* 151 (Hvattum, 2002), so **34** was tentatively identified as eriodictyol-*O*-dihexoside. Compound **62**, with $[M-H]^-$ ion at *m*/*z* 449, was tentatively characterized as eriodictyol-*O*-hexoside.

Compounds **35** displayed $[M-H]^-$ ion at *m*/*z* 415 and, after a neutral loss of 162 Da, yielded the aglycone daidzein at *m*/*z* 253 (Kang et al., 2007), so it was tentatively characterized as daidzein-*O*-hexoside. Compound **48**, followed a similar fragmentation pattern after loss of 46 Da;it was also tentatively identified as daidzein-*O*-hexoside (formate adduct) and compound **77**, with $[M-H]^-$ at *m*/*z* 253, as daidzein.

Five naringenin derivatives were identified in the extracts. In all cases, the aglycone was observed at *m*/*z* 271, with typical fragment ions at *m*/*z* 151 and 107, indicating naringenin (Chanforan et al., 2012). Compound **36** displayed the 433 → 271 transition and was tentatively characterized as a derivative of naringenin-*O*-hexoside. Compound **53**, with $[M-H]^-$ at *m*/*z* 595, suffered consecutive losses of two hexosides, yielding MS^2 and MS^3 fragment ions at *m*/*z* 433 and 271, respectively, so it was tentatively characterized as naringenin-*O*-dihexoside. Compound **60**, with $[M-H]^-$ at *m*/*z* 681, presented a neutral loss of 204 Da (acetylhexoside) in MS^3 [681 → 475] to yield naringenin, and was tentatively characterized as a derivative of naringenin-*O*-acetylhexoside. Compounds **83** and **104**, with $[M-H]^-$ at *m*/*z* 433, suffered the neutral loss of a hexoside moiety, and were tentatively identified as naringenin-*O*-hexoside. The aglycone naringenin was attributed to compound **121**.

Compounds **43**, **50**, and **57** displayed $[M-H+HCOOH]^-$ at *m*/*z* 491 and suffered the neutral loss of 208 Da (hexoside + formate) to yield the base peak at *m*/*z* 283. This fragment might correspond to glycitein or biochanin A. However, the absence of a product ion

at *m/z* 224 is corroborative with glycitein aglycone (Kang et al., 2007). Thus, these compounds were tentatively characterized as isomers of glycitein-*O*-hexoside. Compounds **69** and **101** exhibited the deprotonated molecular ions at *m/z* 283 and were tentatively characterized as glycitein isomers.

Compounds **49**, **70**, and **91**, with $[M-H]^-$ at *m/z* 447, lost 162 Da in MS^2, yielding the base peak at *m/z* 285 (aglycone). The MS^3 [447 → 285] fragmentation displayed a fragment ion at *m/z* 241, characteristic from luteolin. Hence, they were tentatively identified as luteolin-*O*-hexoside isomers. Compound **61**, with $[M-H]^-$ at *m/z* 767, displayed MS^n fragment ions at *m/z* 447, 429, 327, 309, and 299, which are typical from luteolin-6-*C*-h*exo*side (isoorientin) (Llorent-Martinez et al., 2015), so it was tentatively characterized as a derivative. Compound **68** was tentatively characterized as luteolin-8-*C*-(3-hydroxy-3-methylglutaryl)h*exo*side due to the absence of an ion at *m/z* 429 $[M-H-18]^-$, characteristic from the 6-*C* hexoside. The loss of 144 Da corresponds to a 3-hydroxy-3-methylglutaryl moiety (Montoro et al., 2013).

Many liquiritigenin derivatives were found in the methanolic extracts of leaves and flowers. Compound **54**, with $[M-H]^-$ at *m/z* 579, suffered the neutral losses of two hexosides, yielding liquiritigenin at *m/z* 255 (Wang et al., 2008), so it was tentatively characterized as liquiritigenin-*O*-dihexoside. Compounds **59**, **65**, **76**, **103**, and **105** displayed the deprotonated molecular ion at *m/z* 417, and suffered the neutral loss of 162 Da, yielding liquiritigenin. Compound **65** was identified as liquiritin (liquiritigenin-4′-*O*-glucoside) by comparison with a commercial standard. Compounds **59**, **76**, **103**, and **105** were tentatively characterized as liquiritin isomers. Compound **78** displayed the deprotonated molecular ion at *m/z* 621 and suffered neutral losses of 162 Da and 204 Da, so it was tentatively characterized as liquiritigenin-*O*-hexoside-*O*-acetylhexoside. Compounds **47**, **67**, **79**, **88**, **93**, and **99** also presented liquiritigenin fragment ions in their fragmentation patterns, and were tentatively characterized as derivatives. It is important to mention that liquiritigenin and isoliquiritigenin present the same fragmentation patterns (Wang et al., 2008); therefore, some of the compounds may be liquiritigenin or isoliquiritigenin derivatives. Compounds **86** and **117**, with $[M-H]^-$ ion at *m/z* 459, suffered the neutral loss of 204 Da, yielding the aglycone liquiritigenin, so they were tentatively characterized as liquiritigenin-*O*-acetylhexoside. Compound **127** displayed the $[M-H]^-$ ion at *m/z* 255 and was tentatively characterized as liquiritigenin.

Compound **75** exhibited $[M-H+HCOOH]^-$ ion at *m/z* 507 and, after losing 46 Da (formate), displayed a fragmentation pattern previously described for trihidroxy-methoxyl flavanone-*O*-hexoside (Qiao et al., 2011).

Compounds **81** and **106**, with $[M-H]^-$ at *m/z* 505, suffered the neutral loss of 204 Da (acetylhexoside) to yield quercetin and were tentatively characterized as quercetin-*O*-acetylhexoside isomers.

Compound **82** displayed the deprotonated molecular ion at *m/z* 447 and suffered the neutral loss of 162 Da, yielding the aglycone kaempferol at *m/z* 285, so it was tentatively identified as kaempferol-*O*-hexoside. Compound **109** exhibited $[M-H]^-$ at *m/z* 489 and, after the loss of 204 Da, yielded kaempferol. Compound **112** was identified as kaempferol, with $[M-H]^-$ at *m/z* 285 and typical fragment ions at *m/z* 257, 229 and 151 (comparison with an analytical standard).

Compound **85** presented the deprotonated molecular ion at *m/z* 431 and, after the loss of a hexoside moiety, yielded the aglycone at *m/z* 269, which was identified as genistein (Kang et al., 2007). Hence, **85** was tentatively characterized as genistin (genistein-*O*-hexoside).

Compound **98** displayed the $[M+HCOOH-H]^-$ ion at *m/z* 475, and the $[M-H]^-$ ion was observed in MS^2 at *m/z* 429. The fragmentation pattern of this compound exhibited the neutral loss of 162 Da (429 → 267). The aglycone at *m/z* 267 was attributed to formononetin (Kang et al., 2007), hence, **98** was tentatively characterized as formononetin-*O*-hexoside. Compound **115** was tentatively identified as formononetin.

Prunetin-*O*-hexoside and prunetin-*O*-acetylhexoside were attributed to compounds **110** and **120**, with $[M-H+HCOOH]^-$ and $[M-H]^-$ at *m/z* 491 and 487, respectively, since the aglycone was observed at *m/z* 283 and its 283 → 255 transition matches the pattern previously described in literature for prunetin (Aisyah et al., 2013).

Compound **119** exhibited $[M-H]^-$ ion at *m/z* 313 with fragment ions at *m/z* 298 $[M-H-CH_3]^-$, 283 $[M-H-2CH_3]^-$, 269 $[M-H-CO_2]^-$ and 255 $[M-H-CO_2-CH_3]^-$. Thus, **119** was tentatively characterized as 5,4′-dihydroxy-3,7-dimethoxyflavone (Wang et al., 2008).

3.3. Other compounds

Compounds **1** and **2** were tentatively characterized as oligosaccharides considering bibliographic data (Llorent-Martinez et al., 2015).

Compound **5** was tentatively identified as citric acid, considering its $[M-H]^-$ ion at *m/z* 191, and the characteristic base peak at *m/z* 111 (Spínola et al., 2014).

Compound **30**, with $[M-H+HCOOH]^-$ at *m/z* 431, suffered the neutral loss of 46 Da (formate) to yield an ion at *m/z* 385, which was tentatively identified as roseoside considering bibliographic data (Spínola et al., 2014).

Based on previous data (Ye et al., 2005), compound **58** was tentatively identified as a derivative of 4-methyl-3-methoxy-9α-hydroxyligballinol.

Compound **72** displayed $[M-H]^-$ at *m/z* 519, and suffered a hexoside loss to yield the MS^2 base peak at *m/z* 357. The ion at *m/z* 357 matched pinoresinol considering bibliographic data (Eklund et al., 2008), so **72** was tentatively characterized as pinoresinol-*O*-hexoside.

Compounds **92** and **94**, with $[M-H]^-$ at *m/z* 621 and 591, respectively, (Table 1) suffered the neutral loss of 204 Da, yielding fragment ions at *m/z* 417 and 387, respectively. The fragment ion at *m/z* 417 was identified as syringaresinol, whereas the ion at *m/z* 387 corresponded to medioresinol (Eklund et al., 2008). Thus, **92** and **94** were tentatively characterized as syringaresinol-*O*-acetylhexoside and medioresinol-*O*-acetylhexoside, respectively.

Compounds **116**, **118**, **125**, **128**, and **129** were tentatively characterized as saponins comparing the experimental fragmentation patterns observed with those reported in bibliography for other saponins (Pollier et al., 2011).

3.4. Quantification of individual polyphenols

In total, 61 main polyphenols present in *U. europaeus* were quantified by an HPLC-DAD method (Table 2). It was not possible to quantify all the identified compounds due to their low UV-absorption and/or low concentrations.

The phenolic composition of different morphological parts varied qualitatively and quantitatively, being the flowers a richer source of these phytochemicals. Significant differences ($p < 0.05$) were observed in TIPC between morphological parts.

The results indicated that flavones, flavanones, and flavonols were the dominant class of compounds in the leaves and flowers of *Ulex*, which is corroborant with the LC–MS screening. Moreover, leaves and flowers collected in Funchal had higher concentrations of polyphenols than Machico counterparts. However, no significant differences ($p < 0.05$) were found among flowers counterparts.

Hydroxycinnamic acids were residual components in the methanol extracts, more abundant in flowers than leaves but

Table 1
Compounds found in leaves and flowers of *Ulex europaeus* collect at two different locations of Madeira Island (F: Funchal; M: Machico).

N°	t_R (min)	$[M-H]^-$ (m/z)	HPLC-DAD-ESI/MS^n m/z (% base peak)	Assigned identity	Morphological part	Ref.
1	3.0	473	MS^2 [473]: 427 (16), 341 (100), 179 (28), 131 (34) MS^3 [473 → 341]: 179 (100), 161 (18), 143 (17), 131 (22), 113 (15), 101 (25) MS^4 [473 → 341 → 179]: 161 (55), 143 (90), 119 (28), 113 (20), 89 (100)	Oligosaccharide (pentose + dihexose)	Flowers M, F	–
2	3.3	683	MS^2 [683]: 342 (12.0), 341 (100) MS^3 [683 → 341]: 179 (100), 161 (19), 113 (37), 131 (16) 119 (13), 101 (18) MS^4 [683 → 341 → 179]: 161 (23), 149 (20), 143 (34), 119 (22), 89 (100)	Hexose polymer	All	Llorent-Martinez et al. (2015)
3	3.8	525	MS^2 [525]: 262 (100) MS^3 [525 → 262]: 218 (23), 202 (98), 200 (32), 158 (100), 142 (39), 96 (52) MS^4 [525 → 262 → 158]: 96 (100)	Unknown	Flowers M	–
4	4.0	643	MS^2 [643]: 626 (22), 625 (100), 539 (44), 497 (19), 478 (34), 303 (24) MS^3 [643 → 625]: 497 (34), 480 (34), 479 (100), 467 (12), 437 (36), 321 (25), 303 (23), 175 (35) MS^4 [643 → 625 → 479]: 520 (93), 321 (11), 303 (100), 175 (42)	Unknown	Leaves M, FFlowers M	–
5	4.3	191	MS^2 [191]: 173 (12), 111 (100)	Citric acid	All	Spínola et al. (2014)
6	4.6	461	MS^2 [461]: 329 (88), 167 (100), 152 (18) MS^3 [461 → 167]: 152 (100), 123 (93), 108 (31) MS^4 [461 → 167 → 123]: 109 (100) MS^4 [461 → 167 → 152]: 108 (100)	Vanillic acid 4-pentosylhexoside	All	–
7	4.8	503	MS^2 [503]: 341 (100), 179 (48) MS^3 [503 → 341]: 179 (100) MS^4 [503 → 341 → 179]: 135 (100)	Caffeic acid-*O*-dihexoside	Flowers M, F	–
8	5.2	653	MS^2 [653]: 446 (16), 445 (100) MS^3 [653 → 445]: 283 (100), 282 (38), 268 (10) MS^4 [653 → 445 → 283]: 269 (12), 268 (100), 267 (12), 240 (11)	Acacetin-*O*-dihexoside (formate adduct)	All	–
9	5.5	623	MS^2 [623]: 416 (18), 415 (100) MS^3 [623 → 415]: 295 (11), 253 (59), 252 (100) MS^4 [623 → 415 → 253]: 225 (35), 209 (100), 208 (95)	Daidzein-*O*-dihexoside (formate adduct)	All	–
10	5.8	341	MS^2 [341]: 179 (100), 135 (22) MS^3 [341 → 179]: 135 (100)	Caffeic acid-*O*-hexoside	Flowers M, F	Gouveia and Castilho (2009)
11	6.0	371	MS^2 [371]: 325 (19), 163 (100) MS^3 [371 → 163]: 119 (100)	Coumaric acid-O-hexoside (formate adduct)	Leaves M, F	–
12	6.2	447	MS^2 [447]: 315 (40), 271 (32), 207 (36), 179 (26), 163 (68), 161 (46), 152 (100) MS^3 [447 → 152]: 124 (100), 123 (75), 108 (83)	Unknown	Leaves M, F	–
13	6.3	625	MS^2 [625]: 463 (100), 462 (16), 301 (47) MS^3 [625 → 463]: 302 (17), 301 (100), 300 (52), 299 (47), 271 (12) MS^4 [625 → 463 → 301]: 299 (24), 272 (32), 271 (100), 255 (33), 254 (11), 227 (17), 179 (58), 151 (55)	Quercetin-*O*-dihexoside	Flowers M, F	Gouveia and Castilho (2009)

Table 1 (*Continued*)

N°	t_R (min)	[M−H]$^-$ (m/z)	HPLC-DAD-ESI/MS^n m/z (% base peak)	Assigned identity	Morphological part	Ref.
14	6.5	593	MS^2 [593]: 474 (20), 473 (100) MS^3 [593 → 473]: 445 (69), 311 (27), 310 (44), 283 (33), 282 (100) MS^4 [593 → 473 → 282]: 267 (59), 253 (43), 239 (39), 238 (100)	Unknown	Leaves M, F	–
15	6.6	681	MS^2 [681]: 555 (27), 411 (25), 393 (31), 349 (12), 309 (39), 267 (100), 249 (54) MS^3 [681 → 267]: 250 (18), 249 (91), 207 (18), 131 (10), 129 (16), 113 (100), 95 (37), 85 (73) MS^4 [681 → 267 → 249]: 231 (100)	Unknown	Leaves M, F	–
16	6.9	711	MS^2 [711]: 625 (16), 355 (100) MS^3 [711 → 355]: 193 (100) MS^4 [711 → 355 → 193]: 178 (95), 150 (26), 149 (77), 134 (100)	Ferulic acid-*O*-hexoside dimer	Flowers M, F	Fang et al. (2002)
17	7.1	609	MS^2 [609]: 447 (100), 285 (52) MS^3 [609 → 447]: 285 (100) MS^4 [609 → 447 → 285]: 257 (100), 185 (11)	Kaempferol-*O*-dihexoside	All	Ye et al. (2005)
18	7.0	465	MS^2 [465]: 303 (100), 285 (37) MS^3 [465 → 303]: 286 (16), 285 (100), 177 (16), 125 (18) MS^4 [465 → 303 → 285]: 243 (14), 242 (16), 241 (84), 199 (14), 175 (100)	Taxifolin-*O*-hexoside	Flowers M, F	Hashim et al. (2013)
19	7.3	431	MS^2 [431]: 369 (48), 329 (100), 203 (60), 191 (13), 179 (22), 125 (68) MS^3 [431 → 329]: 269 (51), 203 (100), 167 (21), 125 (83), 107 (21) MS^3 [431 → 369]: 333 (19), 243 (100), 165 (36), 163 (24), 125 (43) MS^4 [431 → 329 → 125]: 97 (100)	Unknown	Leaves M, F	–
20	7.5	341	MS^2 [341]: 179 (100), 135 (22) MS^3 [341 → 179]: 135 (100)	Caffeic acid-*O*-hexoside	All	Gouveia and Castilho (2009)
21	7.7	639	MS^2 [639]: 593 (3), 473 (2), 432 (21), 431 (100) MS^3 [639 → 431]: 269 (50), 268 (100) MS^4 [639 → 431 → 268]: 267 (32), 240 (49), 239 (59), 224 (100), 212 (23), 201 (19), 196 (24)	Apigenin-*C*-hexoside-*O*-hexoside (formate adduct)	All	Yang et al. (2011)
22	7.9	609	MS^2 [609]: 448 (19), 447 (100), 285 (54) MS^3 [609 → 447]: 286 (12), 285 (100) MS^4 [609 → 447 → 285]: 283 (13), 257 (100), 255 (10), 230 (12), 229 (21), 217 (12)	Kaempferol-O-dihexoside	Flowers M, F	Ye et al. (2005)
23	8.0	651	MS^2 [651]: 325 (100) MS^3 [651 → 325]: 163 (100), 119 (26) MS^4 [651 → 325 → 163]: 119 (100)	Coumaric acid-*O*-hexoside dimer	Flowers M, F	Sánchez-Rabaneda et al. (2003)
24	8.1	507	MS^2 [507]: 461 (100), 299 (34.6) MS^3 [507 → 461]: 299 (100) MS^4 [507 → 461 → 299]: 284 (100)	3′5,7-trihydroxyisoflavone-4′-methoxy-3′-*O*-β-glucopyranoside (formate adduct)	Flowers M	Ma et al. (2014)
25	8.3	205	MS^2 [205]: 159 (26), 143 (40), 115 (100) MS^3 [205 → 115]: 115 (42), 85(100), 58 (64)	Unknown	Leaves M, FFlowers M	–
26	8.4	487	MS^2 [487]: 355 (16), 337 (26), 217 (18), 193 (100), 149 (19) MS^3 [487 → 193]: 178 (75), 149 (63), 134 (199)	Ferulic acid-*O*-pentosylhexoside	Leaves F	–

Table 1 (*Continued*)

N°	t_R (min)	[M−H]$^-$ (m/z)	HPLC-DAD-ESI/MS^n m/z (% base peak)	Assigned identity	Morphological part	Ref.
27	8.6	669	MS^2 [669]: 623 (18.8), 462 (21.3), 461 (100) MS^3 [669 → 461]: 298 (100), 297 (49.4), 283 (16.7), 269 (14.7) MS^4 [669 → 461 → 299]: 284 (100), 270 (10.3), 269 (56.4), 176 (15.9)	3′5,7-trihydroxyisoflavone-4′-methoxy-3′-*O*-β-diglucopyranoside (formate adduct)	Flowers M, F	–
28	8.6	531	MS^2 [531]: 295 (18), 235 (60), 193 (100) MS^3 [531 → 193]: 149 (17), 134 (100)	Ferulic acid derivative	Leaves M, F	–
29	8.9	711	MS^2 [711]: 668 (30), 667 (100) MS^3 [711 → 667]: 506 (15), 505 (100), 463 (23), 462 (26), 301 (39) MS^4 [711 → 667 → 505]: 344 (15), 323 (12), 301 (19), 300 (100), 271 (27)	Quercetin-*O*-hexoside-*O*-malonyl(hexoside)	Flowers M, F	Gouveia and Castilho (2009)
30	9.0	431	MS^2 [431]: 386 (18), 385 (100), 223 (16), 153 (11) MS^3 [431 → 385]: 223 (48), 205 (55), 161 (24), 154 (14), 153 (100)	Roseoside (formate adduct)	Leaves M, FFlowers M	Spínola et al. (2014)
31	9.0	355	MS^2 [355]: 193 (100) MS^3 [355 → 193]: 178 (39), 149 (100), 134 (77)	Ferulic acid-*O*-hexoside	Flowers M, F	Fang et al. (2002)
32	9.5	341	MS^2 [341]: 179 (100), 135 (22) MS^3 [341 → 179]: 135 (100)	Caffeic acid-*O*-hexoside	Flowers M, F	Gouveia and Castilho (2009)
33	9.6	449	MS^2 [449]: 421 (9), 327 (12), 288 (12), 287 (100), 259 (21) MS^3 [449 → 287]: 260 (17), 259 (100), 243 (17)	Dihydrokaempferol-*O*-hexoside	All	Llorent-Martinez et al. (2015)
34	9.8	611	MS^2 [611]: 450 (20), 449 (100), 287 (13) MS^3 [611 → 449]: 287 (100), 151 (24) MS^4 [611 → 449 → 287]: 151 (100)	Eriodictyol-*O*-dihexoside	Flowers M	–
35	10.0	415	MS^2 [415]: 254 (13), 253 (100), 252 (57) MS^3 [415 → 253]: 288 (42), 252 (44), 225 (60), 224 (100), 223 (31), 208 (77)	Daidzein-*O*-hexoside	Flowers M, F	–
36	10.2	631	MS^2 [631]: 433 (100), 271 (24) MS^3 [631 → 433]: 271 (100) MS^4 [631 → 433 → 271]: 177 (15), 152 (19), 151 (100), 107 (14)	Naringenin-*O*-hexoside derivative	Flowers M, F	–
37	10.3	355	MS^2 [355]: 337 (8), 295 (78), 265 (100), 235 (63), 193 (37) MS^3 [355 → 265]: 193 (100), 149 (10), 134 (15) MS^4 [355 → 265 → 193]: 178 (71), 149 (78), 134 (100)	Ferulic acid-6-*C*-hexoside	Leaves F	–
38	10.5	537	MS^2 [537]: 489 (19), 328 (23), 327 (100) MS^3 [537 → 327]: 313 (26), 312 (100), 164 (22), 149 (10) MS^4 [537 → 327 → 312]: 283 (89), 281 (17), 151 (12), 149 (22), 149 (100)	Unknown	Leaves M, F	–
39	10.5	385	MS^2 [385]: 325 (65), 295 (100), 265 (82), 223 (25) MS^3 [385 → 295]: 224 (22), 223 (100) MS^4 [385 → 295 → 223]: 209 (63), 208 (100), 165 (21), 163 (42)	Sinapic acid-*C*-hexoside	Leaves F	Vallverdú-Queralt et al. (2014)
40	10.8	711	MS^2 [711]: 667 (100) MS^3 [711 → 667]: 505 (100), 504 (44), 463 (63), 301 (68) MS^4 [711 → 667 → 505]: 301 (100), 299 (33)	Quercetin-*O*-hexoside-*O*-malonyl(hexoside)	Flowers M, F	Gouveia and Castilho (2009)
41	11.1	459	MS^2 [459]: 265 (12), 235 (18), 193 (100), 175 (57) MS^3 [459 → 193]: 149 (41), 134 (100)	Ferulic acid derivative	Leaves M, F	–
42	11.5	355	MS^2 [355]: 295 (62), 265 (100), 235 (77), 193 (32) MS^3 [355 → 265]: 193 (100) MS^4 [355 → 265 → 193]: 178 (72), 149 (100), 134 (49)	Ferulic acid-8-*C*-hexoside	Leaves F Flowers M, F	–
43	11.8	491	MS^2 [491]: 445 (18), 284 (16), 283 (100) MS^3 [491 → 283]: 269 (16), 268 (100), 140 (13) MS^4 [491 → 283 → 268]: 241 (14), 240 (100)	Glycitein-*O*-hexoside (formate adduct)	All	–

Table 1 (*Continued*)

N°	t_R (min)	$[M-H]^-$ (m/z)	HPLC-DAD-ESI/MS^n m/z (% base peak)	Assigned identity	Morphological part	Ref.
44	12.6	625	MS^2 [625]: 464 (24), 463 (100), 301 (15) MS^3 [625 → 463]: 302 (18), 301 (100), MS^4 [625 → 463 → 301]: 273 (25), 243 (10), 229 (31), 179 (100), 151 (28)	Quercetin-*O*-dihexoside	All	–
45	12.7	551	MS^2 [551]: 491 (88), 461 (37), 431 (50), 389 (100) MS^3 [551 → 389]: 193 (100), 149 (11), 134 (59) MS^4 [551 → 389 → 193]: 178 (100), 149 (96), 134 (9)	Ferulic acid-*C*-hexoside derivative	Leaves F	–
46	12.7	475	MS^2 [475]: 430 (18), 429 (100), 163 (29) MS^3 [475 → 429]: 265 (17), 163 (100) MS^4 [475 → 429 → 163]: 145 (41), 119 (56), 103 (100), 101 (53), 89 (24)	Coumaric acid derivative (formate adduct)	Leaves M, F	–
47	12.8	665	MS^2 [665]: 459 (31), 417 (100) MS^3 [665 → 417]: 256 (15), 255 (100) MS^4 [665 → 417 → 255]: 153 (15), 135 (100)	Liquiritigenin derivative	All	–
48	13.0	461	MS^2 [461]: 416 (11), 415 (39), 254 (16), 253 (100) MS^3 [461 → 253]: 253 (100), 224 (80), 211 (82), 197 (93), 180 (89), 135 (59)	Daidzein-*O*-hexoside (formate adduct)	All	–
49	13.5	447	MS^2 [447]: 286 (16), 285 (100) MS^3 [447 → 285]: 257 (100), 243 (10), 241 (31), 229 (18), 217 (16)	Luteolin-*O*-hexoside	All	Qiao et al. (2011)
50	13.8	491	MS^3 [491]: 445 (23), 284 (20), 283 (100) MS^3 [491 → 283]: 269 (16), 268 (100) MS^4 [491 → 283 → 268]: 240 (100), 239 (48), 212 (10), 211 (15), 196 (30)	Glycitein-*O*-hexoside (formate adduct)	Leaves M, FFlowers M	–
51	14.0	431	MS^2 [431]: 269 (58), 268 (100) MS^3 [431 → 268]: 240 (76), 239 (64), 224 (100), 223 (28), 212 (24)	Apigenin-*O*-hexoside	All	Qiao et al. (2011)
52	14.1	567	MS^2 [567]: 405 (17), 358 (30), 357 (100) MS^3 [567 → 357]: 343 (22), 342 (100), MS^4 [567 → 357 → 342]: 328 (66), 327 (39), 313 (100), 312 (59), 150 (43), 149 (56)	Unknown	Leaves M, F	–
53	14.2	595	MS^2 [595]: 433 (100), 271 (13) MS^3 [595 → 433]: 271 (100), 151 (26) MS^4 [595 → 433 → 271]: 227 (10), 177 (12), 165 (10), 151 (100), 107 (27)	Naringenin-*O*-dihexoside	Flowers M	Chanforan et al. (2012)
54	14.5	579	MS^2 [579]: 418 (17), 417 (100), 255 (28) MS^3 [579 → 417]: 256 (10), 255 (100) MS^4 [579 → 417 → 255]: 153 (34), 135 (100), 119 (35)	Liquiritigenin-*O*-dihexoside	All	–
55	15.0	461	MS^2 [461]: 342 (17), 341 (100) MS^3 [461 → 341]: 326 (100), 313 (53), 298 (67) MS^4 [461 → 341 → 326]: 299 (13), 298 (100)	Unknown	Leaves F Flowers M, F	–
56	15.0	463	MS^2 [463]: 343 (18), 301 (100), 283 (15), 151 (27) MS^3 [463 → 301]: 257 (12), 241 (42), 211 (11), 179 (26), 169 (15), 151 (100)	Quercetin-*O*-hexoside	Flowers M	–
57	15.3	491	MS^2 [491]: 445 (29), 284 (14), 283 (100) MS^3 [491 → 283]: 269 (16), 268 (100), 240 (9) MS^4 [491 → 283 → 268]: 241 (28), 240 (100)	Glycitein-*O*-hexoside (formate adduct)	Leaves M, F Flowers F	–
58	15.5	565	MS^2 [565]: 340 (19), 339 (100), 328 (11), 327 (47) MS^3 [565 → 339]: 325 (18), 324 (100), 309 (12) MS^4 [565 → 339 → 324]: 309 (100)	4-Methyl-3-methoxy-9α-hydroxyligballinol derivative	All	Ye et al. (2005)

Table 1 (*Continued*)

N°	t_R (min)	$[M-H]^-$ (m/z)	HPLC-DAD-ESI/MS^n m/z (% base peak)	Assigned identity	Morphological part	Ref.
59	15.8	417	MS^2 [417]: 255 (100) MS^3 [417 → 255]: 153 (29), 135 (100), 119 (14)	Liquiritin isomer	Flowers M, F	Wang et al. (2008)
60	16.1	681	MS^2 [681]: 475 (100), 433 (17) MS^3 [681 → 475]: 271 (100) MS^4 [681 → 475 → 271]: 177 (23), 151 (100)	Naringenin-*O*-acetylhexoside derivative	Flowers M	–
61	16.3	767	MS^2 [767]: 539 (26), 490 (10), 489 (43), 447 (46), 429 (35), 357 (20), 327 (100) MS^3 [767 → 327]: 300 (23), 299 (100), 284 (29), 309 (10) MS^4 [767 → 327 → 299]: 297 (29), 255 (100), 232 (32), 213 (15)	Luteolin-6-*C*-hexoside (isoorientin) derivative	Leaves M, F	–
62	16.3	449	MS^2 [449]: 287 (100) MS^3 [449 → 287]: 151 (100), 135 (11)	Eriodictyol-*O*-hexoside	Flowers M	Hvattum (2002)
63	16.6	679	MS^2 [679]: 517 (100), 323 (16) MS^3 [679 → 517]: 323 (100), 179 (18) MS^4 [679 → 517 → 323]: 233 (22), 203 (21), 179 (100), 161 (36), 149 (44), 135 (20)	Caffeic acid derivative	Flowers M	–
64	17.2	609	MS^2 [609]: 343 (15), 301 (100), 300 (21) MS^3 [609 → 301]: 271 (29), 179 (100), 151 (36)	Rutin	Flowers M, F	standard
65	17.7	417	MS^2 [417]: 255 (100) MS^3 [417 → 255]: 154 (13), 153 (50), 135 (100), 119 (24)	Liquiritin	All	standard
66	17.8	711	MS^2 [711]: 667 (100), 505 (41), 463 (13) MS^3 [711 → 667]: 505 (92), 463 (100), 301 (36) MS^4 [711 → 667 → 463]: 301 (100), 179 (19)	Quercetin-*O*-hexoside-*O*-malonyl(hexoside)	Flowers M	Gouveia and Castilho (2009)
67	18.2	751	MS^2 [751]: 459 (100) MS^3 [751 → 459]: 255 (100) MS^4 [751 → 459 → 255]: 153 (48), 135 (100), 119 (32)	Liquiritigenin-*O*-acetylhexoside derivative	Flowers M	–
68	18.9	591	MS^2 [591]: 447 (33), 393 (47), 369 (18), 357 (100), 327 (56) MS^3 [591 → 357]: 339 (35), 298 (16), 297 (100), 285 (66) MS^4 [591 → 357 → 297]: 269 (85), 255 (83), 253 (100), 241 (30), 225 (41)	Luteolin-8-*C*-(hydroxy-3-methylglutaryl)hexoside	Leaves M, F	–
69	19.4	283	MS^2 [283]: 269 (33), 268 (100), 249 (12) MS^3 [283 → 268]: 24 (42), 240 (100) MS^4 [283 → 268 → 240]: 212 (64), 196 (100), 195 (70), 184 (27)	Glycitein isomer	Leaves M	Kang et al. (2007)
70	19.5	447	MS^2 [447]: 286 (14), 285 (100) MS^3 [447 → 285]: 241 (100), 227 (43), 143 (40), 151 (23)	Luteolin-*O*-hexoside	Leaves F	Qiao et al. (2011)
71	20.0	463	MS^2 [463]: 301 (100) MS^3 [463 → 301]: 271 (10), 255 (10), 193 (14), 179 (100), 152 (15), 151 (86)	Quercetin-*O*-hexoside	All	–
72	20.0	519	MS^2 [519]: 358 (16), 357 (100) MS^3 [519 → 357]: 136 (28), 151 (100) MS^4 [519 → 357 → 151]: 136 (100), 107 (23)	Pinoresinol-*O*-hexoside	Leaves M, F	Ye et al. (2005)
73	20.7	477	MS^2 [477]: 432 (20), 431 (100), 269 (37) MS^3 [477 → 431]: 269 (83), 268 (100) MS^4 [477 → 431 → 268]: 240 (100), 239 (77), 224 (96), 223 (59)	Apigenin-*O*-hexoside (formate adduct)	All	Qiao et al. (2011)
74	21.5	427	MS^2 [427]: 383 (11), 365 (23), 325 (100), 222 (13), 221 (38), 161 (84), 149 (35), 143 (59), 131 (18), 125 (59) MS^3 [427 → 325]: 221 (100), 161 (64), 113 (71) MS^4 [427 → 325 → 221]: 161 (100)	Unknown	Leaves M, F	–
75	21.7	507	MS^2 [507]: 462 (27), 461 (100), 300 (14), 299 (90) MS^3 [507 → 461]: 446 (100), 299 (75), 298 (68), 297 (25), 283 (21), 269 (6) MS^4 [507 → 461 → 446]: 284 (34), 283 (100), 255 (20)	Trihidroxy-methoxylflavanone-*O*-hexoside	All	Qiao et al. (2011)
76	23.2	417	MS^2 [417]: 255 (100) MS^3 [417 → 255]: 153 (10), 135 (100), 119 (24)	Liquiritin isomer	Flowers M, F	Wang et al. (2008)
77	23.5	253	MS^2 [253]: 224 (100), 209 (44), 135 (59)	Daidzein	All	Kang et al. (2007)

Table 1 (*Continued*)

N°	t_R (min)	$[M-H]^-$ (m/z)	HPLC-DAD-ESI/MS^n m/z (% base peak)	Assigned identity	Morphological part	Ref.
78	23.5	621	MS^2 [621]: 459 (100), 417 (32), 255 (27) MS^3 [621 → 459]: 255 (100) MS^4 [621 → 459 → 255]: 135 (100), 119 (24)	Liquiritigenin-*O*-hexoside-*O*-acetylhexoside	Leaves F Flowers M, F	–
79	24.4	665	MS^2 [665]: 622 (14), 621 (58), 460 (21), 459 (100), 417 (42) MS^3 [665 → 459]: 255 (100) MS^4 [665 → 459 → 255]: 153 (33), 135 (100), 229 (20), 91 (16)	Liquiritigenin derivative	All	–
80	25.3	575	MS^2 [575]: 513 (32), 473 (18), 432 (16), 431 (100), 341 (58), 311 (55) MS^3 [575 → 431]: 311 (100) MS^4 [575 → 431 → 311]: 284 (16), 283 (100)	Apigenin-*C*-hexoside derivative	Leaves M, F	–
81	25.4	505	MS^2 [505]: 463 (33), 445 (15), 343 (10), 301 (100), 271 (14) MS^3 [505 → 301]: 271 (52), 255 (43), 179 (100), 151 (90), 121 (12)	Quercetin-*O*-acetylhexoside	Flowers M, F	–
82	25.4	447	MS^2 [447]: 284 (100) MS^3 [447 → 284]: 267 (14), 255 (100), 239 (16), 229 (27), 223 (16), 164 (24), 163 (10), 133 (14)	Kaempferol-*O*-hexoside	Flowers M	Spínola et al. (2014)
83	26.0	433	MS^2 [433]: 271 (100) MS^3 [433 → 271]: 151 (100), 107 (15) MS^4 [433 → 271 → 151]: 169 (52), 122 (36), 107 (100), 65 (60)	Naringenin-*O*-hexoside	All	Chanforan et al. (2012)
84	26.4	515	MS^2 [515]: 353 (100) MS^3 [515 → 353]: 191 (100), 179 (46), 135 (11) MS^4 [515 → 353 → 191]: 173 (86), 171 (58), 155 (62), 153 (16), 145 (21), 137 (39), 127 (100), 112 (17), 111 (50), 93 (66), 85 (79), 71 (26)	3,5-*O*-Dicaffeoylquinic acid	Leaves M	Sánchez-Rabaneda et al. (2003)
85	26.7	431	MS^2 [431]: 271 (11), 269 (55), 268 (100) MS^3 [431 → 268]: 240 (60), 239 (100), 224 (99), 223 (49), 196 (23)	Genistin	All	
86	27.4	459	MS^2 [459]: 255 (100) MS^3 [459 → 255]: 153 (50), 136 (10), 135 (100), 119 (47), 91 (10)	Liquiritigenin-*O*-acetylhexoside	Leaves MFlowers M, F	–
87	27.7	577	MS^2 [577]: 455 (14), 370 (20), 369 (100) MS^3 [577 → 369]: 351 (29), 294 (23), 293 (100) MS^4 [577 → 369 → 293]: 293 (33), 265 (41), 251 (26), 222 (28), 175 (100), 173 (79), 164 (16), 118 (17)	Unknown	Leaves M, F	–
88	27.8	503	MS^2 [503]: 459 (100) MS^3 [503 → 459]: 255 (100) MS^4 [503 → 459 → 255]: 153 (48), 135 (100), 119 (40)	Liquiritigenin derivative	Flowers M, F	–
89	28	463	MS^2 [463]: 302 (17), 301 (100) MS^3 [463 → 301]: 257 (17), 179 (86), 151 (100), 121 (8), 107 (5)	Quercetin-*O*-hexoside	Leaves F,Flowers M, F	–
90	28.3	845	MS^2 [845]: 719 (23), 515 (11), 473 (50), 431 (54), 413 (32), 311 (100), 283 (32) MS^3 [845 → 311]: 284 (15), 283 (100)	Apigenin-C-hexoside derivative	Leaves M, F	–
91	28.4	447	MS^2 [447]: 285 (100) MS^3 [447 → 285]: 257 (25), 241 (20), 169 (35), 151 (100), 107 (15)	Luteolin-*O*-hexoside	Flowers M, F	Qiao et al. (2011)
92	28.5	621	MS^2 [621]: 417 (100) MS^3 [621 → 417]: 402 (21), 182 (12), 181 (100), 166 (66), 151 (27) MS^4 [621 → 417 → 181]: 166 (100)	Syringaresinol-*O*-acetylhexoside	Leaves M, F	–
93	28.6	835	MS^2 [835]: 673 (100), 417 (40), 255 (78) MS^3 [835 → 673]: 417 (18), 255 (100) MS^4 [835 → 673 → 255]: 153 (11), 135 (100)	Liquiritigenin derivative	Flowers F	Wang et al. (2008)

Table 1 (*Continued*)

N°	t_R (min)	[M−H]$^-$ (m/z)	HPLC-DAD-ESI/MS^n m/z (% base peak)	Assigned identity	Morphological part	Ref.
94	29.0	591	MS^2 [591]: 387 (100) MS^3 [591 → 387]: 372 (31), 181 (100), 166 (29), 151 (84), 136 (25) MS^4 [591 → 387 → 181]: 166 (100)	Medioresinol-*O*-acetylhexoside	Leaves M, F	–
95	29.9	439	MS^2 [439]: 231 (100) MS^3 [439 → 231]: 187 (100) MS^4 [439 → 231 → 187]: 132 (100)	Unknown	Flowers M, F	–
96	29.9	463	MS^2 [463]: 301 (100) MS^3 [463 → 301]: 193 (13), 179 (99), 151 (100)	Quercetin-*O*-hexoside	Flowers M, F	–
97	30.0	617	MS^2 [617]: 557 (22), 515 (27), 494 (17), 475 (11), 473 (80), 395 (100) MS^3 [617 → 395]: 378 (13), 377 (100), 349 (12), 213 (11), 161 (17) MS^4 [617 → 395 → 377]: 349 (61), 333 (100), 283 (73), 239 (16), 215 (90)	Unknown	Leaves M, F	–
98	30.7	475	MS^2 [475]: 429 (2), 268 (17), 267 (100) MS^3 [475 → 267]: 253 (17), 252 (100) MS^4 [475 → 267 → 252]: 224 (100), 223 (86), 209 (36), 208 (80), 132 (14)	Formononetin-*O*-hexoside (formate adduct)	All	
99	31.2	751	MS^2 [751]: 459 (100), 255 (12) MS^3 [751 → 459]: 255 (100) MS^4 [751 → 459 → 255]: 153 (24), 135 (100)	Liquiritigenin-*O*-acetylhexoside derivative	All	–
100	31.3	269	MS^2 [269]: 241 (100), 223 (69); 214 (30), 201 (57), 197 (63), 196 (49) MS^3 [269 → 241]: 197 (100)	Unknown	All	–
101	31.6	283	MS^2 [283]: 268 (100), 240 (20) MS^3 [283 → 268]: 241 (19), 240 (100) MS^4 [283 → 268 → 240]: 196 (12), 184 (100)	Glycitein isomer	Leaves M, F	Kang et al. (2007)
102	31.8	675	MS^2 [675]: 531 (11), 411 (12), 394 (20), 393 (100) MS^3 [675 → 393]: 365 (54), 351 (86), 283 (23), 257 (44), 239 (29), 215 (90), 133 (100)	Unknown	Leaves F	–
103	31.9	417	MS^2 [417]: 255 (100) MS^3 [417 → 255]: 153 (30), 135 (100), 119 (22)	Liquiritin isomer	All	(Wang et al., (2008)
104	32.3	433	MS^2 [433]: 271 (100) MS^3 [433 → 271]: 177 (22), 151 (100) MS^4 [433 → 271 → 151]: 107 (100)	Naringenin-*O*-hexoside	Flowers M	Chanforan et al. (2012)
105	32.5	417	MS^2 [417]: 255 (100) MS^3 [417 → 255]: 153 (44), 135 (100)	Liquiritin isomer	All	Wang et al. (2008)
106	32.7	505	MS^2 [505]: 301 (100) MS^3 [505 → 301]: 257 (10), 179 (96), 151 (100), 107 (11)	Quercetin-*O*-acetylhexoside	Flowers M, F	–
107	32.8	515	MS^2 [515]: 353 (100) MS^3 [515 → 353]: 335 (14), 283 (28), 282 (100), 281 (58) MS^4 [515 → 353 → 282]: 253 (66), 238 (28), 163 (37), 161 (100)	Unknown	Leaves M, F	–
108	33.5	253	MS^2 [253]: 224 (73), 208 (100), 199 (32), 153 (56), 135 (24), 133 (30), 91 (43)	Unknown	Flowers M, F	–
109	33.7	489	MS^2 [489]: 285 (100) MS^3 [489 → 285]: 257 (17), 169 (10), 151 (100), 107 (12)	Kaempferol-*O*-acetylhexoside	Flowers M, F	–
110	34.2	491	MS^2 [491]: 445 (32), 284 (25), 283 (100) MS^3 [491 → 283]: 268 (27), 255 (100), 213 (17), 151 (18)	Prunetin-*O*-hexoside (formate adduct)	Leaves M, F	Aisyah et al. (2013)
111	34.3	591	MS^2 [591]: 385 (41), 223 (100), 205 (56), 180 (20) MS^3 [591 → 223]: 208 (36), 164 (100), 149 (42)	Sinapic acid derivative	Leaves M, F	–
112	34.9	285	MS^2 [285]: 257 (100), 151 (44) MS^3 [285 → 257]: 239 (67), 230 (47), 229 (100)	Kaempferol	Flowers M, F	standard
113	35.1	367	MS^2 [367]: 205 (22), 179 (100), 135 (14) MS^3 [367 → 179]: 135 (100)	Caffeic acid derivative	Flowers M	–

Table 1 (*Continued*)

N°	t_R (min)	$[M-H]^-$ (m/z)	HPLC-DAD-ESI/MS^n m/z (% base peak)	Assigned identity	Morphological part	Ref.
114	35.2	659	MS^2 [659]: 597 (36), 537 (41),515 (47), 455 (40), 395 (74), 377 (100) MS^3[659 → 377]: 349 (100), 335 (23), 333 (24), 283 (23), 239 (16), 215 (56) MS^4 [659 → 377 → 349]: 334 (38), 321 (82), 269 (100)	Unknown	Leaves M, F	–
115	35.4	267	MS^2 [267]: 252 (100) MS^3 [267 → 252]: 223 (100), 208 (69), 195 (46), 133 (17)	Formononetin	Flowers M, F	Kang et al. (2007)
116	36.0	973.5	MS^2 [974]: 955 (100), 911 (28), 809 (2) 783 (5), 765 (37), 665 (2), 647 (43), 629 (26), 603 (31), 557 (73), 489 (32) MS^3 [974 → 956]: 911 (51), 765 (48), 629 (30), 557 (100), 489 (17) MS^4 [974 → 955 → 557]: 507 (80), 489 (6), 439 (100), 409 (51)	Saponin-1	All	Pollier et al. (2011)
117	36.4	459	MS^2 [459]: 255 (100) MS^3 [459 → 255]: 153 (62), 136 (10), 135 (100), 119 (33), 91 (12)	Liquiritigenin-*O*-acetylhexoside	All	–
118	36.5	827.5	MS^2 [828]: 665 (9), 648 (20), 647 (100), 629 (15), 603 (37), 557 (31), 489 (49) MS^3 [828 → 647]: 615 (100), 559 (60), 490 (44), 489 (59), 441 (44) MS^4 [828 → 647 → 615]: 597 (25), 585 (78), 570 (14), 545 (100), 457 (53)	Saponin-2	All	Pollier et al. (2011)
119	37.7	313	MS^2 [313]: 298 (100) MS^3 [313 → 298]: 283 (40.8), 269 (100), 255 (20.4), 242 (49.2), 241 (34.2), 200 (22.0), 161 (37.4), 131 (17.8) MS^4 [313 → 298 → 269]: 255 (15.9), 253 (12.5), 242 (25.8), 241 (47.6), 227 (24.1), 201 (47.2), 200 (47.5), 197 (100), 161 (18.5)	5,4′-dihydroxy-3,7-dimethoxyflavone	Leaves M	Wang et al. (2008)
120	38.1	487	MS^2 [487]: 284 (14), 283 (100) MS^3 [487 → 283]: 255 (100), 254 (37) MS^4 [487 → 283 → 255]: 241 (100), 227 (63), 213 (56), 212 (76), 209 (48), 157 (68)	Prunetin-*O*-acetylhexoside	Leaves FFlowers M	–
121	39.2	271	MS^2 [271]: 177 (24), 151 (100) MS^3 [271 → 151]: 107 (100), 83 (12)	Naringenin	Flowers M, F	Chanforan et al. (2012)
122	39.4	687	MS^2 [687]: 641 (100) MS^3 [687 → 641]: 480 (32), 479 (100) MS^4 [687 → 641 → 479]: 317 (11), 161 (100)	Unknown	Leaves M, F	–
123	39.6	269	MS^2 [269]: 253 (40), 233 (37), 227 (23), 225 (100), 201 (23), 197 (57), 151 (44) MS^3 [269 → 225]: 181 (100)	Apigenin	Flowers M, F	Qiao et al. (2011)
124	39.9	351	MS^2 [351]:163 (100), 119 (18) MS^3 [351 → 163]: 119 (100)	Coumaric acid derivative	Leaves M, F	–
125	40.4	957.5	MS^2 [957]: 939 (100), 895 (30), 811 (13), 767 (6), 749 (36), 631 (32), 613 (26), 541 (59), 473 (13), 453 (10) MS^3 [957 → 939]: 921 (38), 895 (18), 749 (36), 613 (5), 541 (100), 473 (8) MS^4 [957 → 939 → 541]: 499 (32), 455 (100)	Saponin-3	All	Pollier et al. (2011)
126	40.8	381	MS^2 [381]: 193 (100), 134 (10), 115 (15) MS^3 [381 → 193]: 178 (57), 149 (100), 134 (61)	Ferulic acid derivative	Leaves M, F	–
127	43.5	255	MS^2 [255]: 153 (39), 135 (100), 119 (22) MS^3 [255 → 135]: 153 (100), 91 (14)	Liquiritigenin	Flowers M, F	Wang et al. (2008)
128	44.7	941.5	MS^2 [942]: 923 (100), 879 (30), 795 (22), 751 (7), 733 (36), 615 (26), 597 (28), 525 (62), 457 (25) MS^3 [942 → 923]: 879 (24), 733 (26), 597 (32), 525 (100)	Saponin-4	All	Pollier et al. (2011)
129	46.1	795.5	MS^2 [795]: 633 (25), 615 (100), 525 (56), 457 (25) MS^3 [795 → 615]: 571 (48), 553 (68), 497 (76), 457 (100), 451 (27)	Saponin-5	Leaves M, F	Pollier et al. (2011)

Table 2
Quantification of the main polyphenolic compounds present in leaves and flowers of *Ulex europaeus* (mg per 100 g DE).

			Leaves		Flowers	
N°	MW	*Hydroxycinnamic acids*	*Machico*	*Funchal*	*Machico*	*Funchal*
7	503	Caffeic acid-*O*-dihexoside	–	–	17.03 ± 0.53	19.43 ± 0.37
20	341	Caffeic acid-*O*-hexoside	27.38 ± 1.76	31.89 ± 1.80	64.17 ± 2.13	90.68 ± 3.06
32	341	Caffeic acid-*O*-hexoside	–	–	84.89 ± 3.79	92.52 ± 4.13
84	515	3,5-*O*-Dicaffeyolquinic acid	42.57 ± 2.78	–	–	–
28	531	Ferulic acid derivative	1.88 ± 0.11	6.77 ± 0.22	–	–
37	355	Ferulic acid-6-*C*-hexoside	–	23.18 ± 1.07	–	–
41	459	Ferulic acid derivative	–	2.68 ± 0.17	–	–
45	551	Ferulic acid-*C*-hexoside derivative	–	3.34 ± 0.21	–	–
11	371	Coumaric acid-*O*-hexoside	8.21 ± 0.34	10.33 ± 0.41	–	–
23	651	Coumaric acid-*O*-hexoside dimer	–	–	47.45 ± 3.23	139.36 ± 9.14
46	475	Coumaric acid derivative	38.86 ± 2.16	43.64 ± 2.77	–	–
124	351	Coumaric acid derivative	14.93 ± 0.94	–	16.71 ± 1.11	–
111	591	Sinapic acid derivative	3.58 ± 0.09	9.22 ± 1.11	–	–
		Total	137.39 ± 8.18	151.05 ± 7.79	280.36 ± 8.07	342.00 ± 51.34
		Hydroxybenzoicacids				
6	461	Vanillic acid 4-hexosylpentoside	25.37 ± 1.09	34.55 ± 1.20	42.12 ± 1.54	47.09 ± 1.38
		Total	25.37 ± 1.09	34.55 ± 1.20	42.12 ± 1.54	47.09 ± 1.38
		Flavonols				
13	625	Quercetin-*O*-dihexoside	–	–	864.25 ± 11.75	887.77 ± 14.76
29	711	Quercetin-*O*-hexoside-*O*-malonyl(hexoside)	–	–	92.34 ± 3.36	107.37 ± 4.45
40	711	Quercetin-*O*-hexoside-*O*-malonyl(hexoside)			25.00 ± 1.36	35.20 ± 2.05
44	625	Quercetin-*O*-dihexoside			311.21 ± 8.64	333.47 ± 9.03
56	463	Quercetin-*O*-hexoside	21.00 ± 0.63	24.45 ± 0.94	594.45 ± 5.64	627.23 ± 4.73
81	505	Quercetin-*O*-acetylhexoside	–	–	17.8 ± 0.75	21.48 ± 0.71
96	463	Quercetin-*O*-hexoside isomer	–	–	986.65 ± 43.01	1023.57 ± 48.32
106	505	Quercetin-*O*-acetylhexoside isomer	–	–	48.34 ± 1.33	63.08 ± 1.89
17	609	Kaempferol-*O*-dihexoside	241.85 ± 13.78	281.23 ± 12.90	426.29 ± 14.55	456.59 ± 11.39
33	449	Dihydrokaempferol-*O*-hexoside	242.72 ± 9.45	258.93 ± 8.99	301.60 ± 10.11	325.01 ± 9.76
82	447	Kaempferol-*O*-hexoside	55.13 ± 1.97	57.34 ± 2.04	55.17 ± 3.35	64.64 ± 3.12
		Total	560.71 ± 25.83	621.96 ± 26.12	3723.10 ± 198.41	3989.40 ± 254.66
		Flavones				
8	653	Acacetin-*O*-diglucoside	107.12 ± 3.32	115.16 ± 3.65	126.71 ± 4.35	135.36 ± 4.77
21	639	Apigenin-*C*-hexoside-*O*-hexoside	521.89 ± 4.56	562.50 ± 5.21	1396.32 ± 43.74	1854.62 ± 54.23
49	447	Luteolin-*O*-hexoside	55.32 ± 3.65	67.82 ± 2.82	267.26 ± 10.22	297.90 ± 9.75
51	431	Apigenin-*O*-hexoside	77.84 ± 2.55	107.14 ± 3.44	170.34 ± 9.41	200.58 ± 8.56
73	477	Apigenin-*O*-hexoside	232.07 ± 7.53	244.49 ± 7.01	654.72 ± 10.35	770.33 ± 12.49
80	575	Apigenin-*C*-hexoside derivative	21.92 ± 1.62	38.69 ± 1.88	–	–
90	845	Apigenin-*C*-hexoside derivative	40.17 ± 2.33	42.83 ± 2.99	–	–
123	269	Apigenin	–	–	16.77 ± 1.42	17.94 ± 2.15
		Total	1056.83 ± 77.43	1178.63 ± 79.33	2632.12 ± 186.73	3276.73 ± 235.11
		Isoflavones				
9	623	Daidzin-*O*-dilhexoside	99.87 ± 2.9	116.37 ± 2.1	214.70 ± 5.70	250.16 ± 5.63
24	507	3′5,7-trihydroxyisoflavone-4′-methoxy-3′-O-β-glucopyranoside	–	–	159.21 ± 3.12	166.37 ± 3.24

Table 2 (*Continued*)

N°	MW	*Hydroxycinnamic acids*	Leaves		Flowers	
			Machico	*Funchal*	*Machico*	*Funchal*
43	491	Glycitin isomer	1027.11 ± 55.1	1234.53 ± 53.88	1596.06 ± 53.78	1654.33 ± 50.01
48	461	Daidzein-*O*-hexoside	179.59 ± 4.11	219.35 ± 3.77	569.84 ± 27.41	695.99 ± 26.44
50	491	Glycitin isomer	33.59 ± 2.23	–	39.28 ± 1.78	41.27 ± 1.84
69	283	Glycitein	14.03 ± 0.39	–	–	–
77	253	Daidzein	45.99 ± 1.45	48.80 ± 0.99	74.31 ± 3.73	77.93 ± 2.99
85	431	Genistin	7.83 ± 0.46	9.97 ± 0.71	19.82 ± 0.77	20.76 ± 1.11
98	475	Formononetin-*O*-hexoside	15.87 ± 0.99	18.14 ± 1.14	18.87 ± 0.79	23.14 ± 0.95
110	491	Prunetin-*O*-hexoside	1.80 ± 0.09	12.52 ± 0.73	–	–
		Total	1425.68 ± 95.78	1659.68 ± 99.44	2692.05 ± 167.34	2929.95 ± 188.65
		Flavanones				
36	631	Narigenin-*O*-hexoside derivative	–	–	14.05 ± 1.98	17.51 ± 1.64
60	681	Narigenin-*O*-acetylhexoside derivative	–	–	185.45 ± 17.43	–
83	433	Narigenin-*O*-hexoside	115.90 ± 8.14	119.24 ± 6.32	145.45 ± 7.37	159.31 ± 7.01
121	271	Narigenin	–	–	52.19 ± 3.53	54.55 ± 1.12
75	507	Trihidroxy-methoxylflavanone-*O*-glucoside	–	153.30 ± 11.75	318.69 ± 10.99	457.26 ± 17.10
47	665	Liquiritigenin derivative	43.24 ± 2.56	69.35 ± 3.33	63.71 ± 2.95	72.92 ± 2.37
59	417	Liquiritin isomer	–	–	13.28 ± 1.03	17.50 ± 1.17
65	417	Liquiritin[a]	12.67 ± 0.97	16.66 ± 0.81	23.20 ± 22.98	25.75 ± 18.99
76	417	Liquiritin isomer	–	–	496.77 ± 30.39	512.37 ± 35.71
78	621	Liquiritin-*O*-hexoside-*O*-acetylhexoside	–	60.69 ± 6.32	157.29 ± 8.31	170.75 ± 9.92
79	665	Liquiritigenin derivative	214.55 ± 16.09	219.05 ± 15.79	249.52 ± 13.73	297.93 ± 10.35
88	503	Liquiritigenin derivative	–	–	227.67 ± 14.11	249.62 ± 10.74
99	751	Liquiritigenin-*O*-acetylhexoside derivative	602.05 ± 34.08	659.81 ± 27.99	1354.62 ± 86.57	1406.06 ± 97.34
103	417	Liquiritin isomer	256.53 ± 17.03	296.79 ± 19.06	543.87 ± 43.65	589.11 ± 39.35
105	417	Liquiritin isomer	83.60 ± 8.49	102.43 ± 7.25	209.24 ± 26.33	294.00 ± 19.55
117	459	Liquiritigenin-*O*-acetylhexoside	9.69 ± 0.27	16.17 ± 0.53	58.81 ± 4.32	68.19 ± 2.01
127	255	Liquiritigenin	–	–	22.05 ± 1.71	36.22 ± 2.09
		Total	1338.23 ± 110.34	1713.50 ± 108.92	4135.87 ± 285.37	4428.85 ± 255.32
		TIPC	4544.27 ± 334.69	5359.71 ± 313.13	13505.50 ± 1030.42	15013.42 ± 1197.44

[a] Confirmed by commercial standard.

Table 3
Data from TPC, TFC, and *in vitro* antioxidant and enzyme inhibition assays.

	TPC[a]	TFC[b]	DPPH[c]	ABTS[c]	NO[c]	SO[c]	α-Glucosidase[d]	α-Amylase[d]
Leaves Funchal	23.48 ± 1.27	10.74 ± 0.51	111.16 ± 4.2	540.77 ± 11.08	22.21 ± 1.33	15.11 ± 1.04	1.97 ± 0.182	3.36 ± 0.247
Flowers Funchal	30.36 ± 1.41	24.96 ± 1.40	134.30 ± 5.3	660.23 ± 10.31	27.08 ± 1.17	17.15 ± 0.98	1.09 ± 0.086	2.57 ± 0.252
Leaves Machico	22.12 ± 0.99	9.81 ± 0.39	107.11 ± 3.7	531.17 ± 9.88	21.07 ± 1.03	14.05 ± 0.86	2.15 ± 0.157	3.43 ± 0.281
Flowers Machico	28.16 ± 1.16	21.16 ± 0.95	129.22 ± 6.6	653.29 ± 10.97	25.86 ± 1.04	16.85 ± 0.77	1.27 ± 0.091	2.79 ± 0.313
Acarbose	–	–	–	–	–	–	1.619 ± 0.023	0.02 ± 0.002

All measurements are expressed as mean ± SD ($n = 3$).
[a] g GAE/100 g DE.
[b] g QCE/100 g DE.
[c] mmol TE/100 g DE.
[d] IC50 value (mg/mL).

with less diversity. Flavonoids were about three times more abundant in flowers. As shown in Table 2, there was an even distribution of flavonoids amongst four classes: isoflavones (mainly glycitin) < flavones (mainly apigenin derivatives) < flavonols (dominated by quercetin glucosides) < flavanones. Significant differences ($p < 0.05$) were found in isoflavones, flavonols and flavanones contents only among leaves counterparts. The flavanone group was composed largely by derivatives (glucosides) of liquiritigenin; the free aglycone itself was identified in small amounts in flower extracts. All four isomers of liquiritin (liquiritin, isoliquiritin, neoliquiritin and neoisoliquiritin) were detected and quantified. Since their mass spectra are all very similar, exact identification was not attempted and they are described in Tables 1 and 2 as liquiritin isomers. A standard of liquiritin (liquiritigenin-4′-*O*-glucoside) was used, showing that in the extracts of *Ulex*, this was not the most abundant isomer (compound **65**).

Ulex flowers were richer in liquiritigenin derivatives (3740 mg/100 g DE) than the roots and rhizomes of *Glycyrrhiza glabra* L. (about 1242 mg/100 g DE) (Martins et al., 2015), where liquiritigenin apiosides were reported as the main flavonoids, which curiously were absent in *Ulex* extracts. Other authors have presented quantitative results in *Glycyrrhiza* species but expressed

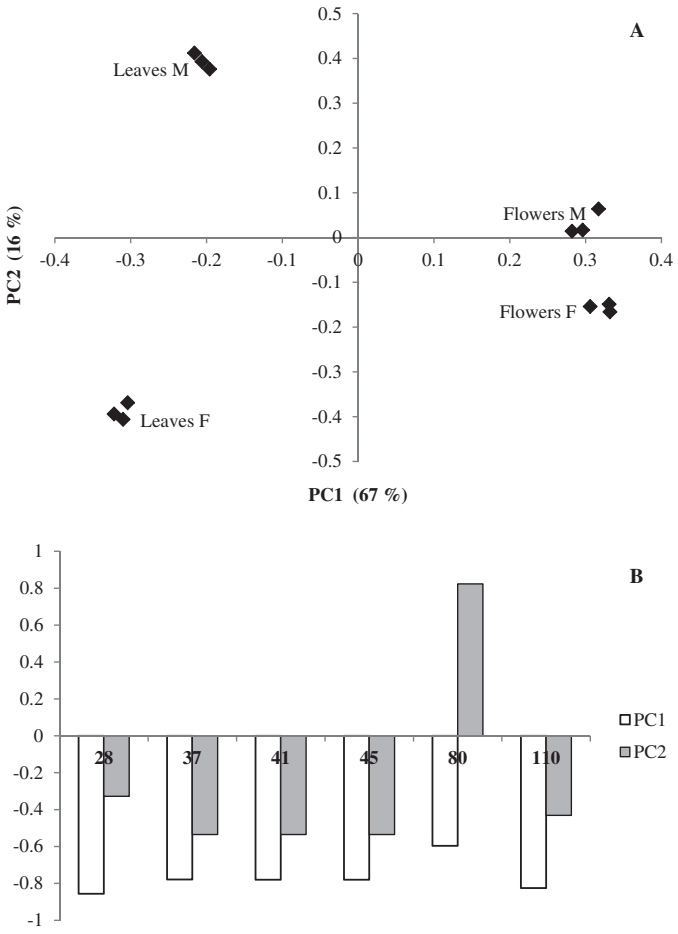

Fig. 3. (A) PC1 × PC2 of scores scatter plot between different *Ulex* morphological parts and collection area; (B) PC1 × PC2 of loading plot of the main source of variability between different *Ulex* morphological parts and collection area.

differently (mg/100 g dry plant, DP). Tian and co-workers (Tian et al., 2009) reported 29 mg/100 DP of liquiritin in commercial liquorice, while in another study (Montoro et al., 2011), liquiritigenin derivatives varied between 1498 and 4049 mg/100 g DP. The latter study presented higher concentrations than *Ulex* flowers (893–1217 mg/100 g DP) analyzed in the present work.

3.5. *TPC, TFC and* in vitro *antioxidant assays*

In the present work, flowers proved to be a better source of phenolic compounds than leaves (Table 3). Moreover, samples from Funchal presented higher TPC and TFC than Machico counterparts, which is in agreement with data shown in Table 2. Significant differences ($p < 0.05$) were found among flower samples in colorimetric determinations.

Overall, the results obtained in the four antioxidant assays revealed *Ulex* good ability to scavenge free radicals (in particular flowers material), which can be partially related to the higher content of polyphenols (Table 3). Under the assay conditions, when comparing collection areas, it is possible to see that Funchal samples presented a stronger antioxidant capacity than Machico counterparts. Significant differences ($p < 0.05$) in the antioxidant activity were observed (except between flower samples in the ABTS assay).

Based on the scavenging capacity observed for both NO and SO tests, *Ulex* might also prevent the formation of other biologically important oxidative species, like peroxynitrite and hydroxyl radical (López-Alarcón and Denicola, 2013; Valko et al., 2007).

These results are corroborative with previous screening and quantification of polyphenols and may justify in part the use of flowers in detriment of leaves in folk medicine (Rivera and Obón, 1995). This variation in the distribution of phenolics may be responsible for the observed biological effects. An explanation for the noticeably higher concentration of polyphenols in Funchal samples may be due to the fact that these were collected at approximately 1400 m high (while Machico at about 600 m). At higher altitudes, plant species are more subject to harsh environmental conditions such as ray from the sunlight or cold. Stress factors may induce intense synthesis of phenolic compounds as a response to abiotic stress in order to prevent oxidative damage of the plant cellular structures.

3.6. *Inhibition of digestive enzymes*

Since *Ulex* was formerly used for the treatment of diabetes and liver diseases (Rivera and Obón, 1995), and liquiritin is described as anti-diabetic (Gaur et al., 2014), the effect of methanolic extracts towards key digestive enzymes linked to type II diabetes was evaluated. *Ulex* samples were more specific inhibitors of α-glucosidase than of α-amylase activities (Table 3). In the α-glucosidase assay, the results showed that flowers presented stronger inhibitory activity than leaves and acarbose. For α-amylase, the same trend was observed, but a weaker inhibition effect compared to the commercial drug acarbose was observed. Statistical differences ($p < 0.05$) were found between acarbose and *Ulex* samples, between morphological parts in all assays and in

the α-glucosidase assay between flowers samples. The inhibition activity could be attributed to the higher content of liquiritigenin derivatives in flowers than in leaves (Table 2). Previous studies (Choi et al., 2010; Gaur et al., 2014) have reported the potent inhibition of liquiritigenin derivatives (neoliquiritin, liquiritin and liquiritigenin) on α-glucosidase, higher than acarbose.

Recently, the inhibitory effects of leaves from *Senna surattensis* (another Fabaceae) on carbohydrate digestive enzymes was studied (Thilagam et al., 2013). Similarly to our results, the extract was found to be more effective inhibiting the activities of α-glucosidases (sucrase and maltase) than α-amylase when compared with acarbose. In another study (Kongstad et al., 2015), six crude extracts from Fabaceae plants were tested for their anti-hyperglycemic activities. Only liquorice and indian tamarind (*Tamarindus indica*) methanolic extracts showed better inhibition of α-glucosidase than acarbose.

3.7. Principal component analysis

PCA statistical tool was applied to the concentrations of 61 polyphenols, in order to establish a relationship between morphological parts and collection area. The PCA score scatter plot of the two first principal components (which explains 83% of the total variability of the HPLC-DAD data set) is shown in Fig. 3A. The loadings of each compound (variable) that contribute to explain the differentiation between the different morphological parts and collection area is shown in Fig. 3B. PC1, that explained 67% of the total variability, shows *Ulex* samples discrimination based on morphological parts, where the leaves are projected in PC1 negative and flowers are above the positive PC2 axis. Taking into account the loading plot (Fig. 3B), the compounds that contribute to these results were ferulic acid derivative (**28**), ferulic acid *C*-hexoside (**37**), apigenin-8-*C*-glucoside derivative (**80**) and prunetin-*O*-hexoside (**110**). On the other hand, PC2 (that explained 16% of the total variability) separated *Ulex* samples based on collection area: Machico samples are above PC2 axis while Funchal counterparts are positioned in PC2 negative. According to Fig. 3B, the polyphenols responsible for the obtained results are ferulic acid derivatives (**28**, **37, 41** and **45**) and prunetin-*O*-hexoside (**110**).

4. Conclusions

The extracts from *Ulex* flowers are very rich in flavonoids, possess high antioxidant activity and present *in vitro* hypoglycemic effects. Using the described HPLC-ESI–MS^n method, 129 compounds were found in the methanolic extracts of leaves and flowers from *U. europaeus*. Flavonoids accounted for over 98% of the components both in flowers and leaves, and were evenly distributed as flavonols, flavones, isoflavones and flavanones, of which the vast majority are liquiritigenin derivatives. Nowadays, there is a new interest in these derivatives, shown by the many recent studies on their pharmacological properties, with most of these studies focused in *Glycyrrhiza* species (Peng et al., 2015). Since several of these liquiritigenin compounds present important biological and pharmacological relevance, it is important to have access to novel, available sources of these chemicals. Here, it has been demonstrated that *Ulex* biomass, especially the flowers, resultant from forest cleaning, can be such a source of valuable polyphenols. This can lead to a new way to look at this plant presently thought of as useless.

Acknowledgments

Spínola is grateful to Fundação para a Ciência e a Tecnologia (FCT, Portugal) for a Ph.D. grant SFRH/BD/84672/2012. E. J. Llorent-Martínez acknowledges the financial support from the UCLM Research Plan. This research was supported by FCT with funds from the Portuguese Government (Project PEst-OE/QUI/UI0674/2013) and the Portuguese National Mass Spectrometry Network (Contract RNEMREDE/1508/REM/2005).

References

Aisyah, S., Gruppen, H., Madzora, B., Vincken, J.-P., 2013. Modulation of isoflavonoid composition of *Rhizopus oryzae* elicited soybean (*Glycine max*) seedlings by light and wounding. J. Agric. Food Chem. 61, 8657–8667.

Chanforan, C., Loonis, M., Mora, N., Caris-Veyrat, C., Dufour, C., 2012. The impact of industrial processing on health-beneficial tomato microconstituents. Food Chem. 134, 1786–1795.

Choi, C.W., Choi, Y.H., Cha, M.-R., Yoo, D.S., Kim, Y.S., Yon, G.H., Hong, K.S., Kim, Y.H., Ryu, S.Y., 2010. Yeast α-glucosidase inhibition by isoflavones from plants of Leguminosae as an *in vitro* alternative to acarbose. J. Agric. Food Chem. 58, 9988–9993.

Eklund, P.C., Backman, M.J., Kronberg, L.A., Smeds, A.I., Sjöholm, R.E., 2008. Identification of lignans by liquid chromatography–electrospray ionization ion-trap mass spectrometry. J. Mass Spectrom. 43, 97–107.

Ewing, J.F., Janero, D.R., 1995. Microplate superoxide dismutase assay employing a nonenzymatic superoxide generator. Anal. Biochem. 232, 243–248.

Fang, N.B., Yu, S.G., Prior, R.L., 2002. LC/MS/MS characterization of phenolic constituents in dried plums. J. Agric. Food Chem. 50, 3579–3585.

Gaur, R., Yadav, K.S., Verma, R.K., Yadav, N.P., Bhakuni, R.S., 2014. In vivo anti-diabetic activity of derivatives of isoliquiritigenin and liquiritigenin. Phytomedicine 21, 415–422.

Gouveia, S.C., Castilho, P.C., 2009. Analysis of phenolic compounds from different morphological parts of Helichrysum devium by liquid chromatography with on-line UV and electrospray ionization mass spectrometric detection. Rapid Commun. Mass Spectrom. 23, 3939–3953.

Harborne, J., 1972. Distribution of flavonoids in the Leguminosae. In: Harborne, J., Boulter, D., Turner, B. (Eds.), Chemotaxonomy of the Leguminosae. Academic Press, London, UK, pp. 31–71.

Hashim, S.N.N.S., Schwarz, L.J., Boysen, R.I., Yang, Y., Danylec, B., Hearn, M.T.W., 2013. Rapid solid-phase extraction and analysis of resveratrol and other polyphenols in red wine. J. Chromatogr. A 1313, 284–290.

Hvattum, E., 2002. Determination of phenolic compounds in rose hip (Rosa canina) using liquid chromatography coupled to electrospray ionisation tandem mass spectrometry and diode-array detection. Rapid Commun. Mass Spectrom. 16, 655–662.

Kang, J., Hick, L.A., Price, W.E., 2007. A fragmentation study of isoflavones in negative electrospray ionization by MSn ion trap mass spectrometry and triple quadrupole mass spectrometry. Rapid Commun. Mass Spectrom. 21, 857–868.

Kongstad, K.T., Özdemir, C., Barzak, A., Wubshet, S.G., Staerk, D., 2015. Combined use of high-resolution α-glucosidase inhibition profiling and high-performance liquid chromatography-high-resolution mass spectrometry-solid-phase extraction-nuclear magnetic resonance spectroscopy for investigation of antidiabetic principles in crude plant extracts. J. Agric. Food Chem. 63, 2257–2263.

López-Alarcón, C., Denicola, A., 2013. Evaluating the antioxidant capacity of natural products: a review on chemical and cellular-based assays. Anal. Chim. Acta 763, 1–10.

Llorent-Martinez, E.J., Spinola, V., Gouveia, S., Castilho, P.C., 2015. HPLC-ESI–MS^n characterization of phenolic compounds terpenoid saponins, and other minor compounds in Bituminaria bituminosa. Ind. Crops Prod. 69, 80–90.

Máximo, P., Lourenço, A., Feio, S.S., Roseiro, J.C., 2000. Flavonoids from Ulex species. Z. für Nat. C 55, 506–510.

Máximo, P., Lourenço, A., Feio, S.S., Roseiro, J.C., 2002a. A new prenylisoflavone from Ulex jussiaei. Z. für Nat. C J. Biosci. 57, 609–613.

Máximo, P., Lourenço, A., Feio, S.S., Roseiro, J.C., 2002b. Flavonoids from Ulex airensis and Ulex europaeus ssp. europaeus. J. Nat. Prod. 65, 175–178.

Ma, Y., Kosińska-Cagnazzo, A., Kerr, W.L., Amarowicz, R., Swanson, R.B., Pegg, R.B., 2014. Separation and characterization of phenolic compounds from dry-blanched peanut skins by liquid chromatography–electrospray ionization mass spectrometry. J. Chromatogr. A 1356, 64–81.

Maier, C., Conrad, J., Carle, R., Weiss, J., Schweiggert, R.M., 2015. Phenolic constituents in commercial aqueous Quillaja (Quillaja saponaria Molina) wood extracts. J. Agric. Food Chem. 63, 1756–1762.

Martins, N., Barros, L., Dueñas, M., Santos-Buelga, C., Ferreira, I.C.F.R., 2015. Characterization of phenolic compounds and antioxidant properties of Glycyrrhiza glabra L. rhizomes and roots. RSC Adv. 5, 26991–26997.

Montoro, P., Maldini, M., Russo, M., Postorino, S., Piacente, S., Pizza, C., 2011. Metabolic profiling of roots of liquorice (Glycyrrhiza glabra) from different geographical areas by ESI/MS/MS and determination of major metabolites by LC–ESI/MS and LC–ESI/MS/MS. J. Pharm. Biomed. Anal. 54, 535–544.

Montoro, P., Teyeb, H., Masullo, M., Mari, A., Douki, W., Piacente, S., 2013. LC–ESI–MS quali-quantitative determination of phenolic constituents in different parts of wild and cultivated Astragalus gombiformis. J. Pharm. Biomed. Anal. 72, 89–98.

Parejo, I., Jauregui, O., Sánchez-Rabaneda, F., Viladomat, F., Bastida, J., Codina, C., 2004. Separation and characterization of phenolic compounds in fennel

(*Foeniculum vulgare*) using liquid chromatography–negative electrospray ionization tandem mass spectrometry. J. Agric. Food Chem. 52, 3679–3687.
Peng, F., Du, Q., Peng, C., Wang, N., Tang, H., Xie, X., Shen, J., Chen, J., 2015. A review: the pharmacology of isoliquiritigenin. Phytother. Res. 29, 969–977.
Podsędek, A., Majewska, I., Redzynia, M., Sosnowska, D., Koziołkiewicz, M., 2014. In vitro inhibitory effect on digestive enzymes and antioxidant potential of commonly consumed fruits. J. Agric. Food Chem. 62, 4610–4617.
Pollier, J., Morreel, K., Geelen, D., Goossens, A., 2011. Metabolite profiling of triterpene saponins in Medicago truncatula hairy roots by liquid chromatography Fourier transform ion cyclotron resonance mass spectrometry. J. Nat. Prod. 74, 1462–1476.
Press, J.R., Short, M.J., 1994. Flora of Madeira. HMSO, London.
Qiao, X., He, W., Xiang, C., Han, J., Wu, L., Guo, D., Ye, M., 2011. Qualitative and quantitative analyses of flavonoids in Spirodela polyrrhiza by high-performance liquid chromatography coupled with mass spectrometry. Phytochem. Anal. 22, 475–483.
Rivera, D., Obón, C., 1995. The ethnopharmacology of Madeira and Porto Santo Islands, a review. J. Ethnopharmacol. 46, 73–93.
Sánchez-Rabaneda, F., Jáuregui, O., Lamuela-Raventós, R.M., Bastida, J., Viladomat, F., Codina, C., 2003. Identification of phenolic compounds in artichoke waste by high-performance liquid chromatography–tandem mass spectrometry. J. Chromatogr. A 1008, 57–72.
Shi, P., Zhang, Y., Qu, H., Fan, X., 2011. Systematic characterisation of secondary metabolites from Ixeris sonchifolia by the combined use of HPLC-TOFMS and HPLC-ITMS. Phytochem. Anal. 22, 66–73.
Sousa, C., Valentão, P., Ferreres, F., Seabra, R.M., Andrade, P.B., 2008. Tronchuda cabbage (Brassica oleracea L: var. costata DC): scavenger of reactive nitrogen species. J. Agric. Food Chem. 56, 4205–4211.
Spínola, V., Llorent-Martínez, E.J., Gouveia, S., Castilho, P.C., 2014. Myrica faya: a new source of antioxidant phytochemicals. J. Agric. Food Chem. 62, 9722–9735.
Thilagam, E., Parimaladevi, B., Kumarappan, C., Mandal, S.C., 2013. α-Glucosidase and α-amylase inhibitory activity of Senna surattensis. J. Acupunct. Meridian Stud. 6, 24–30.
Tian, M., Yan, H., Row, K.H., 2009. Simultaneous extraction and separation of liquiritin glycyrrhizic acid, and glabridin from licorice root with analytical and preparative chromatography. Biotechnol. Bioprocess Eng. 13, 671–676.
Tolera, A., Khazaal, K., Ørskov, E.R., 1997. Nutritive evaluation of some browse species. Anim. Feed Sci. Technol. 67, 181–195.
Valko, M., Leibfritz, D., Moncol, J., Cronin, M.T.D., Mazur, M., Telser, J., 2007. Free radicals and antioxidants in normal physiological functions and human disease. Int. J. Biochem. Cell Biol. 39, 44–84.
Vallverdú-Queralt, A., Regueiro, J., Martínez-Huélamo, M., Rinaldi Alvarenga, J.F., Leal, L.N., Lamuela-Raventos, R.M., 2014. A comprehensive study on the phenolic profile of widely used culinary herbs and spices: rosemary thyme, oregano, cinnamon, cumin and bay. Food Chem. 154, 299–307.
Veitch, N.C., 2007. Isoflavonoids of the leguminosae. Nat. Prod. Rep. 24, 417–464.
Veitch, N.C., 2013. Isoflavonoids of the leguminosae. Nat. Prod. Rep. 30, 988–1027.
Vitale, D.C., Piazza, C., Melilli, B., Drago, F., Salomone, S., 2013. Isoflavones: estrogenic activity, biological effect and bioavailability. Eur. J. Drug Metab. Pharmacokinet. 38, 15–25.
Wang, Y., Yang, L., He, Y.-Q., Wang, C.-H., Welbeck, E.W., Bligh, S.W.A., Wang, Z.-T., 2008. Characterization of fifty-one flavonoids in a chinese herbal prescription Longdan Xiegan Decoction by high-performance liquid chromatography coupled to electrospray ionization tandem mass spectrometry and photodiode array detection. Rapid Commun. Mass Spectrom. 22, 1767–1778.
Waridel, P., Wolfender, J.-L., Ndjoko, K., Hobby, K.R., Major, H.J., Hostettmann, K., 2001. Evaluation of quadrupole time-of-flight tandem mass spectrometry and ion-trap multiple-stage mass spectrometry for the differentiation of C-glycosidic flavonoid isomers. J. Chromatogr. A 926, 29–41.
Yang, H., Ye, X., Liu, D., Chen, J., Zhang, J., Shen, Y., Yu, D., 2011. Characterization of unusual proanthocyanidins in leaves of bayberry (*Myrica rubra* Sieb. et Zucc.). J. Agric. Food Chem. 59, 1622–1629.
Ye, M., Yan, Y., Guo, D.-A., 2005. Characterization of phenolic compounds in the Chinese herbal drug Tu-Si-Zi by liquid chromatography coupled to electrospray ionization mass spectrometry. Rapid Commun. Mass Spectrom. 19, 1469–1484.
Ye, M., Yang, W.-Z., Liu, K.-D., Qiao, X., Li, B.-J., Cheng, J., Feng, J., Guo, D.-A., Zhao, Y.-Y., 2012. Characterization of flavonoids in *Millettia nitida* var. *hirsutissima* by HPLC/DAD/ESI–MS^n. J. Pharm. Anal. 2, 35–42.